Engineering Failure Analysis 157 (2024) 107914

Contents lists available at ScienceDirect

Engineering Failure Analysis

journal homepage: www.elsevier.com/locate/engfailanal

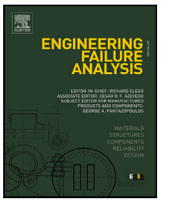

Review

Composite pipelines: Analyzing defects and advancements in non-destructive testing techniques

Muhammad Waqar *, Azhar M. Memon, Muhammad Sabih, Luai M. Alhems

Applied Research Center for Metrology, Standards, and Testing, Research and Innovation, King Fahd University of Petroleum and Minerals, Dhahran, 31261, Eastern Province, Saudi Arabia

ARTICLE INFO

Keywords:
Composites
Defects
Damages
FRP
Non-destructive testing
Pipelines

ABSTRACT

In recent decades, various pipeline industries, such as oil, gas, and water, have increasingly focused on fiber-reinforced polymer (FRP) pipes. This growing interest in FRP pipes offers multiple advantages over traditional pipelines made of steel and concrete, including exceptional corrosion resistance, a favorable weight-to-strength ratio, reduced maintenance costs due to its durability, and customer-specific customization in sizes and strength. However, the intricate manufacturing processes and its specialized handling and installation requirements make it susceptible to defects. The traditional non-destructive testing (NDT) methods, primarily developed for metals, are inadequate when applied to FRP. It is mainly because fiberglass composites are inherently non-homogeneous and anisotropic in contrast to their metallic counterparts, introducing a unique set of challenges. As a result, the fields of Non-destructive Testing & Evaluation (NDT&E) and Structural Health Monitoring (SHM) for FRP piping systems are currently vibrant areas of research and development. The objectives of this paper are (i) to identify potential damage types in composite pipelines, (ii) to compile a comprehensive list of defects currently examined in the literature, and (iii) to present the latest progress in NDT&E techniques for composite pipelines, specifically addressing the operational constraints and practical challenges involved. Consequently, it is tailored specifically to address the needs and challenges of the pipeline sector. It is found that the state of NDT for composite pipelines is still nascent, with extensive research required to reach maturity. Critical areas for development include broadening inspection ranges, validating performance in real-field conditions, detecting, and characterizing natural defects, and improving imaging techniques. Moreover, there is a need to transition from reactive to proactive strategies in pipeline monitoring.

1. Introduction

1.1. Background and motivation

Metallic pipelines are susceptible to corrosion in aggressive environments [1,2], such as those with high humidity and temperature [3]. Corrosion is a significant and commonly occurring defect in metallic pipes. Corroded pipes cause structural degradation and impede the piping system's functionality, resulting in prolonged service downtime, increased maintenance, repair, and operational costs, and reduced service life. Moreover, corroded pipelines carry potential health risks when transporting potable water [4]. As a result, there has been a significant shift within the energy (oil and gas) and water sectors towards non-metallic

* Corresponding author.
E-mail address: muhammad.waqar@kfupm.edu.sa (M. Waqar).

https://doi.org/10.1016/j.engfailanal.2023.107914
Received 15 October 2023; Received in revised form 14 December 2023; Accepted 22 December 2023
Available online 27 December 2023

Nomenclature

λ	Wavelength (m)
ω	Angular frequency (rad s^{-1})
c_g	Group velocity (m s^{-1})
c_p	Phase velocity (m s^{-1})
k	Wavenumber (m^{-1})
t_f	Time-of-flight (s)
x_d	Location of defect (m)
AET	Acoustic emission techniques
ASTM	American Society for Testing and Material
CFRP	Carbon fiber-reinforced polymer
FEA	Finite element analysis
FEM	Finite element modeling
FRP	Fiber-reinforced polymers
GFRP	Glass fiber-reinforced polymer
GRE	Glass fiber-reinforced epoxy resin
GRP	Glass-reinforced polymer
GWUT	Guided waves ultrasonic testing
IRT	Infrared thermography
MWI	Microwave imaging
NDT	Non-destructive testing
NDT&E	NDT & evaluation
PWAS	Piezoelectric wafer active sensors
PZT	Piezoelectric transducers
RTP	Reinforced thermoplastic
RTR	Reinforced thermoset resin
SHM	Structural health monitoring
SNR	Signal-to-noise ratio
VI	Visual inspection

pipes [5]. Non-metallic materials are favored due to their innate resistance to corrosion, tailored performance, lightweight, and lower maintenance and operational costs.

There are various non-metallic materials available for commercial use in piping, including thermoplastics (like polyvinyl chloride (PVC), chlorinated polyvinyl chloride (CPVC), polyethylene, and polypropylene), concrete, rubber, and fiber-reinforced polymer (FRP) (such as carbon fiber-reinforced polymer (CFRP) and glass fiber-reinforced polymer (GRP)). Among these options, GRP has gained popularity in the piping industry due to its exceptional resistance to corrosion, low cost, and favorable suitability for non-conductive applications such as water and wastewater transport [6–8]. It is because typical types of corrosion, such as galvanic, pitting, aerobic, and inter-granular deterioration, do not harm GRP material [9]. Moreover, GRP is suitable for use against various chemicals and temperatures [10]. Another appealing aspect of GRP is that its properties can be customized according to specific requirements, making it even more desirable.

Like any other material, GRP products are also prone to several defects. These defects can potentially arise at various stages throughout the lifespan of GRP, encompassing manufacturing, storage, installation, and in-service operations [11,12]. Fig. 1 provides a comprehensive overview of the spectrum of defects encountered in FRP composites, categorizing them by the stage of occurrence and scale. The defects range from nano-scale imperfections to macro-scale structural issues, highlighting the complexity and variability inherent in composite material behavior. The genesis of these defects can be traced from the manufacturing phase through to the in-service period, with factors such as environmental conditions and mechanical stresses contributing to their development and propagation. This graphical representation synthesizes findings from several key studies [13–18], and it underpins the intricate defect mechanics within FRP products as compared to metals [11,19]. While this figure presents the general and commonly known defects in any composite, the specific defects pertinent to FRP pipelines are discussed in greater detail in Section 4. Each defect depicted has the potential to induce or evolve into other defects, creating a complex web of interactions that can exacerbate material degradation [20]. Unlike the well-defined boundaries of defects in more homogeneous materials (e.g., metals), the defects in FRP can initiate at a minute scale and expand significantly over time. The anisotropic nature of these composites, coupled with their sensitivity to numerous variables—ranging from the matrix composition to the service environment [21–23]—necessitate a thorough understanding of their defect mechanics. Thus, there is a lack of comprehensive understanding, prediction, and prevention of defect development in composites. This knowledge gap highlights the need for further research and advancements in order to better address and mitigate defects in composite materials.

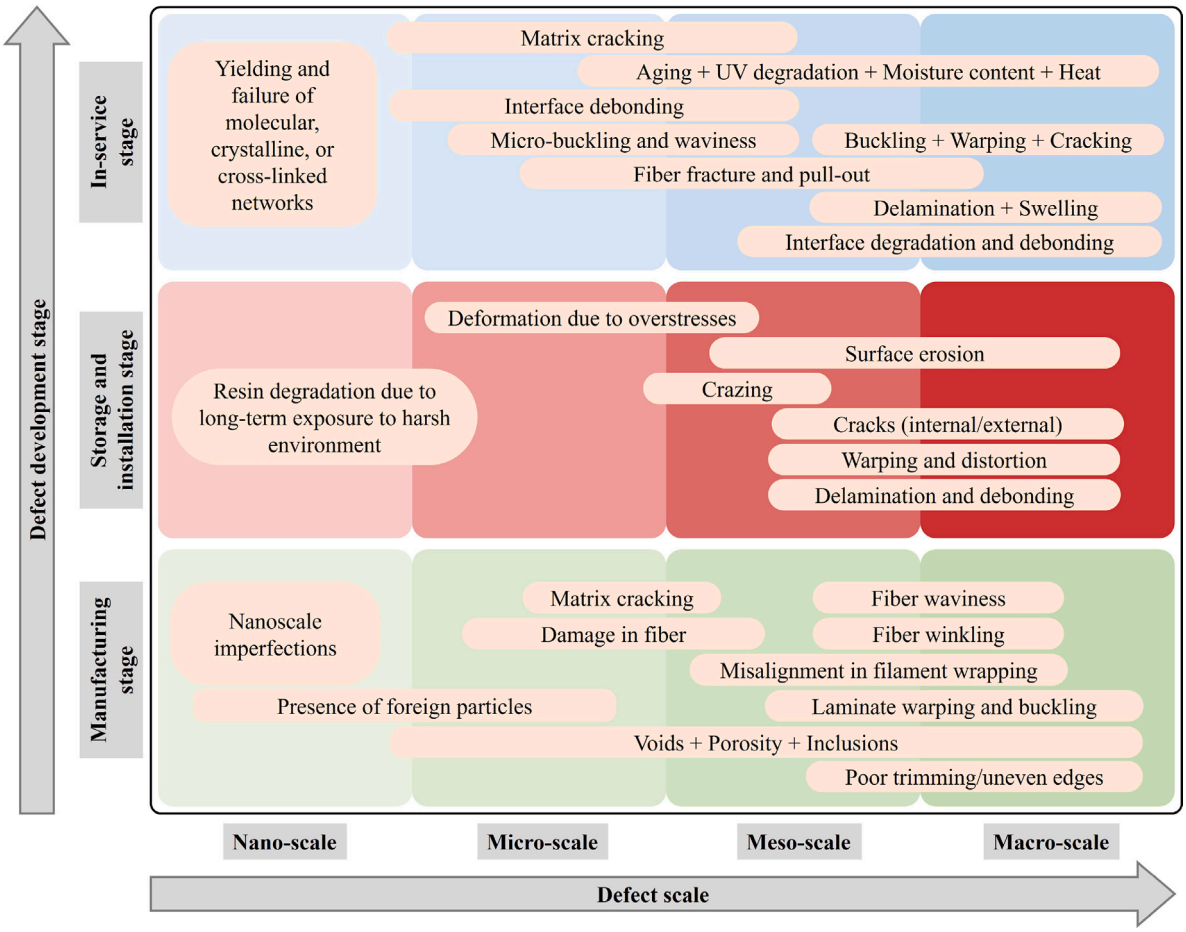

Fig. 1. Defect classification based on their potential scale that may develop in FRP products during manufacturing, storage, installation, and in-service stages.

1.2. Scope of this paper

The development of defect(s) in GRP systems is complex and inevitable. These defects not only hinder the performance and efficiency but may disrupt the system's overall functionality. Therefore, equipment and methods are needed to detect and localize these defects at their early stage of development. In this context, non-destructive testing and evaluation (NDT&E) is a viable and pragmatic solution [24–26]. Over the past few decades, numerous NDT&E techniques have been developed (or upgraded from their applications in metals) to diagnose FRP composites. Fig. 2 provides a list of well-known NDT&E techniques developed for metallic and composite materials. There are different ways to classify other NDT&E techniques, such as classification (i) based on their working requirement (e.g., contact or contact-less), (ii) based on their resolution, and (iii) based on their underlying principles. In Fig. 2, the latter classification is selected to complement the diverse range of techniques based on shared physical principles.

Numerous literature reviews have been published regarding the use of NDT&E techniques for detecting defects in composite materials as outlined in Table 1. It is noticed that most of the existing review papers generally provide a broad overview of NDT&E techniques without specific emphasis on particular fields, with the exception of Garnier et al. [27], which specifically focused on the application of NDT&E in the aeronautical industry. This indicates a clear need for a more targeted review paper on NDT&E for defect detection in pipelines and the pipeline industry. It is because FRP pipelines, unlike other composite products in industries like medicine or aerospace, have unique characteristics such as being out-of-sight (buried underground or off-shore), challenging to access, large in scale (kilometers), complex in design (with valves, junctions, bends, etc.), and operating under demanding conditions (high pressure, significant mass, and large momentum). Consequently, certain NDT&E techniques that are suitable for other applications may not be applicable for diagnosing FRP pipelines, rendering them obsolete.

The motivation of this paper is to conduct a thorough examination of NDT&E techniques specifically tailored for Fiber-Reinforced Polymer (FRP) pipelines. Our approach begins with exploring and discussing a comprehensive list of defects identified in current literature, encompassing their development stages, impacts, and consequences on the durability of FRP pipes. Following this, we delve into the NDT methods developed and documented in scholarly works, reviewing their fundamental principles, application procedures, and requirements and citing relevant works to acknowledge significant contributions in this area. This paper intends

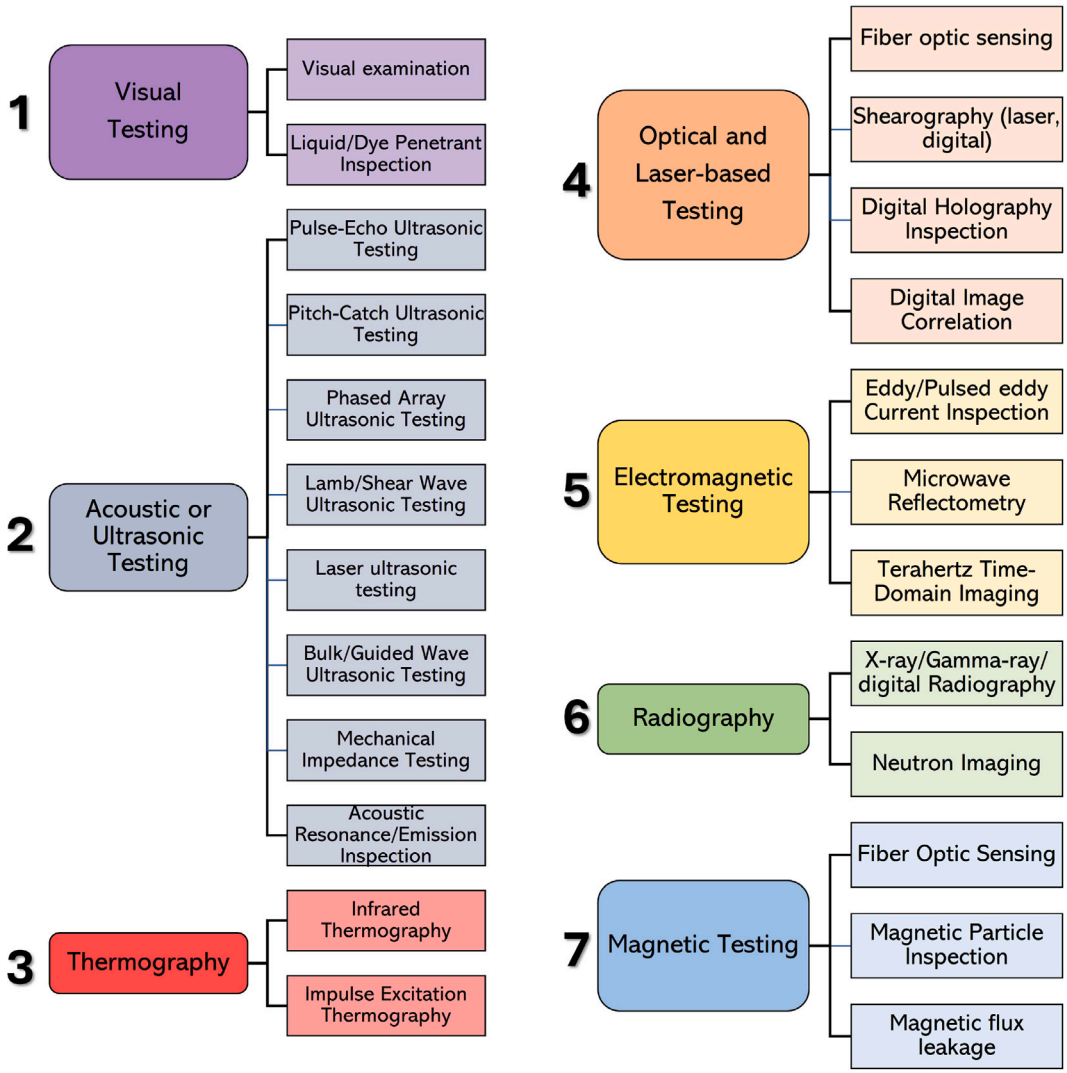

Fig. 2. Classification of various NDT&E techniques used for the inspection and diagnosis of FRP composites.

to provide pipeline engineers and practitioners with informed guidance on selecting appropriate NDT&E techniques suited to their specific needs. Additionally, this paper aims to offer the research community an outlook on the pressing need for future research opportunities, particularly those focused on enhancing pipeline diagnosis and maintenance.

The remaining part of the paper is organized as follows: Section 2 provides a detailed background on FRP composites and their early-stage commercialization. This section also covers FRP pipelines, including their manufacturing processes and potential markets. Section 3 outlines the methodology used to discover the relevant literature (e.g., research articles, patents, white papers, conference proceedings, reports, thesis, etc.) and a bibliometric analysis of the collected material. Section 4 covers reported defects in FRP pipelines, their potential root causes (where available), and their effects on the system's overall functionality. Section 5 discusses the developed NDT&E techniques for pipelines, along with the potential applications of these techniques, their advantages, and limitations. Finally, conclusions and future recommendations are presented.

2. Background on commercial use of FRP

2.1. FRP products

The first commercial utilization of FRP material dates back to 1938 when Owens Corning, an American composite material company, used FRP components for insulation and acoustical isolation [31]. Later, in 1948, it became a viable alternative to metallic piping and was utilized in the crude oil industry. Based on its initial performance, manufacturers began developing

Table 1
Summary of literature review papers on NDT&E techniques.

Review paper	Application domain	Overview
[13]	General review	Reviewed various types of defects in composites, their development, modeling, and progression. Also provided a brief introduction to NDT&E for composites
[15]	General review	Reviewed various NDT&E techniques that can be used to detect defects or damages in composites
[17]	General review	Comprehensive review on NDT&E techniques including their operation requirements, frequency ranges, merits, and limitations
[27]	Domain specific: Aeronautics	Focused on the NDT&E techniques for composite structures used in aeronautical industry. The study focused on ultrasonic testing, infrared thermography, and shearography to diagnose in-service defects in wings and rods
[28]	General review	A brief introduction to several NDT&E techniques, their working principles, and their potential limitations
[29]	General review	Reviewed the fundamentals of guided lamb waves techniques (subclass of Class 2 in Fig. 2) and their applications in examining the composite structures
[30]	General review	Provided a brief description on several NDT&E techniques to examine composite materials

standards and testing methods for FRP products in the 1960s. The demand for FRP products is constantly on the rise, expanding into various sectors such as the aerospace industry [22], automotive manufacturing [32], building & construction [33,34], piping systems for water [35], chemicals [36], oil & gas transport [25], medical [37], and energy harvesting (e.g., wind turbines [38] and hydropower [39]), and many others. Moreover, many organizations publish standards and specifications for FRP products, such as the International Organization for Standardization (ISO), the American Petroleum Institute (API), the American Society of Mechanical Engineers (ASME), the American Society for Testing and Material (ASTM), American Water Works Association (AWWA), British Standards Institution (BSI), and American Composites Manufacturers Association (ACMA). For example, a list of standards from different organizations is provided in Table B.4, which covers GRP pipelines' design and manufacturing aspects in low/high-pressure applications.

2.2. GRP pipelines

The commercial utilization of FRP in the piping industry has experienced significant growth since the introduction of the ISO 14692 standard in 2002 [40] (also mentioned in Table B.4). Currently, the market value of FRP pipes stands at approximately USD 3.7 billion, with projections indicating a growth to USD 6.3 billion by 2030 [41]. FRP pipes are highly versatile and have found applications in many sectors, including (i) water, wastewater, and sewage systems [42,43], (ii) oil and gas industries [44,45], (iii) chemical [7] and desalination plants [46,47]. Fig. 3 presents a list of different types of GRP products based on their polymer type, reinforcing material type, and chemical composition [48–51]. Among several material options (as illustrated in Fig. 3), Glass fiber Reinforced Epoxy resin (GRE—a thermosetting resin material) has a long history in large-scale and high-pressure transmission pipelines [9,35,52,53].

There are several ways to fabricate FRP pipes, including (i) filament winding, (ii) centrifugal casting, (iii) pultrusion, (iv) hand lay-up, and (v) spray-up. Each casting method is briefly described in Appendix A. Among these methods, the filament winding technique is widely used because it offers a controlled and systematic fabrication process [54]. In this method, the fiber is placed in a dual helix arrangement with a specified angle (specified as a positive or negative integer in successive layers) defined concerning the axial direction of the structure. The ply-angle is usually reported as $[\pm\theta^{\circ}]_n$, where n denotes the number of layers (see, for example, Fig. 4). The winding angle plays a significant role in determining the mechanical strength and properties of the final product. Moreover, among the variety of fibers (e.g., glass, carbon, aramid, flax, jute, basalt, and synthetic), glass fibers are frequently used for pipeline manufacturing, with some specialized applications of carbon fiber (such as in high-pressure and high-temperature pipelines). It is because glass fiber-reinforced polymer (GRP) pipes are (i) relatively less expansive than carbon fibers as they are derived from abundant raw materials such as silica sand and limestone, and (ii) their manufacturing process is relatively less complicated than carbon fibers. Table 2 compares the mechanical properties of GRP, CFRP, and other commonly used materials for piping.

3. Methodology for literature survey

The methodology for literature collection is summarized in Fig. 5. A comprehensive literature search was conducted using specific keywords across six databases: (i) Google Scholar, (ii) Scopus (Elsevier), (iii) Google Patents, (iv) United States Patents, (v) Research Gate, and (vi) Web of Science (Clarivate Analytics PLC). The query used to identify relevant records is provided below.

```
TITLE-ABS-KEY((‘‘composite material’’ OR ‘‘reinforced polymer’’)
AND (‘‘fiberglass’’ OR ‘‘glass fiber’’ OR ‘‘GRP’’ OR ‘‘FRP’’ OR ‘‘CFRP’’ OR ‘‘GRP’’)
 AND (‘‘pipe’’ OR ‘‘cylinder’’)
```

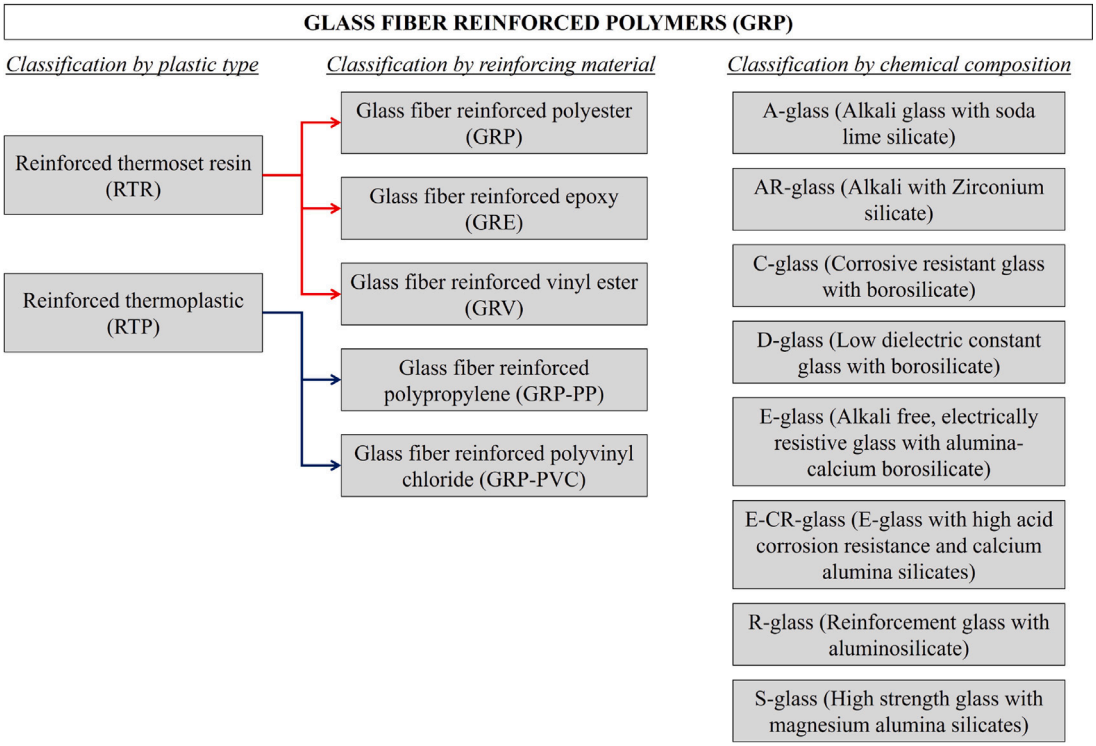

Fig. 3. Classification of GRP products by plastic type (left column) reinforcing material (middle column) and chemical composition (right column).

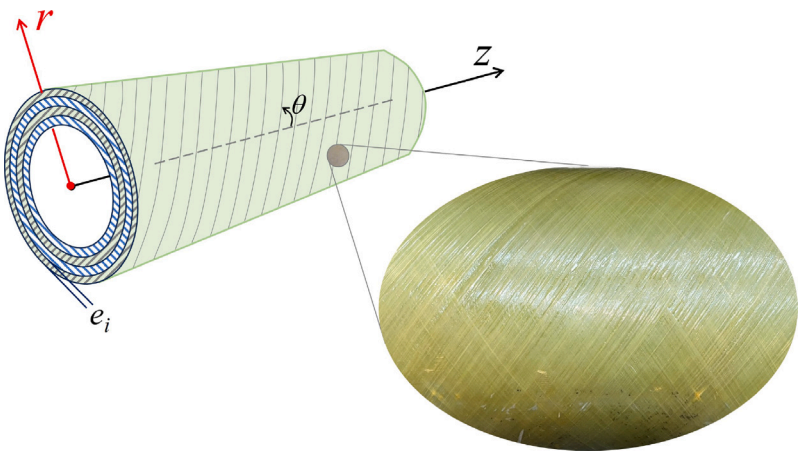

Fig. 4. Multi-layered filament wounded fiberglass pipe with a zoomed patch from a real-life sample, illustrating the ply-angle $[\pm 55^\circ]_{12}$. The symbols (z, r) denote axial and radial coordiantes, and e_i denotes the layer (ply) thickness.

```
AND (''NDT'' OR ''NDE'' OR ''NDT&E'' OR ''defect detection'' OR ''inspection'')
AND (''defect'' OR ''crack'' OR ''delamination'' OR ''leak'')
AND (''technique'' OR ''method'' OR ''methodology'' OR ''analysis'')
AND (''finite element'' OR ''acoustics'' OR ''ultrasonics'' OR ''guided waves'')
```

The foregoing keywords are used individually as well as in various pairs. Different types of literature sources were collected, including journal articles, conference proceedings, patents, PhD dissertations, white papers, technical reports, and review papers. All the relevant records were organized and managed using Zotero (a free and open-source reference management software developed

Table 2
Approximate mechanical properties of GRP and other commonly used materials for pipelines. These values are general estimates and can vary based on the specific grades, classes, or compositions of the materials.

Property (unit)	GRP[a]	CFRP[b]	Steel[c]	Standard concrete[d]	HDPE[e]
Density (g/cm^3)	1.5–2.5	1.8–2.0	≈7.85	≈2.2–2.5	0.93–0.98
Elastic modulus (GPa)	15–75	150–450	200–210	20–40	0.8–1.2
Elongation at break (%)	1–3	0.5–2	5–25	≈0.1	300–600
Poisson's ratio (–)	0.2–0.3	0.2–0.3	≈0.3	0.1–0.2	0.3–0.5
Compressive strength (MPa)	200–600	1500–5200	300–1200	40–80	25–50
Tensile strength (MPa)	2500–4000	3500–6000	400–2000	2–5[f]	20–33
Speed of sound (km/s)	3.0–4.0	3.5–4.5	5.0–6	3.0–4.5	1.5–2.0

[a] Williams (1987) [31]; Cheremisinoff et al. [21]; http://www.mfgil.in/grp-pipes.html.
[b] https://www.goodfellow.com/; https://www.toray.com/global/.
[c] https://www.efunda.com/home.cfm; https://www.matweb.com.
[d] https://www.concretepipe.org/; https://www.astm.org/.
[e] Willoughby 2022 [55]; https://polymerdatabase.com.
[f] Standard concrete has much lower tensile strength than the compressive strength.

by George Mason University [56]). A manual screening process was then conducted to filter further the literature based on the following criteria:

1. **Duplicate entries**: Duplicate articles obtained from different databases were removed to ensure data accuracy.
2. **Full-text unavailability**: Entries behind paywalls or without full-text availability were excluded.
3. **Timeline**: The study primarily focused on published and peer-reviewed articles from 2018 to 2023.
4. **FRP repair in metallic**: Records involving FRP as a repair material for metallic pipelines were separated. While this topic is important and has a significant number of records, its analysis was beyond the scope of this paper and may require a separate analysis.
5. **Material other than GRP**: Most entries involving composites other than GRP were eliminated except for a few papers where GRP was passively discussed.

The purpose of applying the preceding filters was to refine the literature collection and focus on the relevant literature related explicitly to NDT&E of GRP pipelines. As a result, the initial database of 1040 entries was significantly reduced to a final set of 74 entries. Fig. 6 shows the stacked bar plot, indicating the number of shortlisted articles in each document category with respect to publication year. A keyword co-occurrence analysis is performed using the VOSviewer [57] to identify patterns of association among the keywords in the data set. The analysis is performed by creating a map based on the bibliographic data and assigning a minimum keyword occurrence threshold = 3. The analysis shows that, out of 406 keywords, there are 46 keywords that meet the minimum occurrence criterion. The resulting map is displayed in Fig. 7. This figure shows that there are six primary clusters (each with a minimum of 5 keywords), and there are 313 links between different keywords. The following conclusions can be made from this figure:

1. Non-destructive testing of composite materials is a dominant subject, encompassing techniques such as imaging, holography, and microwave measurements.
2. Manufacturing defects [12], particularly delamination and debonding, have received significant attention in the literature.
3. Mathematical modeling for stress analysis and NDT&E is commonly performed using Finite Element Analysis (FEA).

Fig. 8 presents the summary of the study type (analytical, experimental, numerical), and other pipe properties (material, length, internal/nominal diameter, and total wall thickness) from the collected and refined literature database. This figure illustrates that almost 59% of the papers are based on experimental work, indicating the numerical and analytical complexities associated with composite pipes due to their non-homogeneous and anisotropic nature. In terms of study material, GRE (as described in Fig. 3) is the most predominantly studied material, accounting for 38% of the research. It is also noticed that, about 35% of the studies did not specify the type of composite pipe material. This omission is probably due to the samples being sourced from suppliers, with the details assumed to be kept confidential. Moreover, while studies using CFRP and other plastic materials (e.g., PVC and HDPE) are beyond the scope of this paper, they were retained in the final database and analysis. This is because their authors indicated the potential applicability of their techniques to the inspection of GRE pipes.

Pipe samples of shorter lengths (either less than 0.5 m or ranging from 0.5 to 1 m) are mostly used, as they constitute approximately 72% of the dataset. This percentage indicates that many of the developed or considered NDT&E methods focus on short-range applications. Conversely, a limited number of studies, making up just 12% of the data, addressed pipe sections longer than 5 m. With respect to pipe diameter, most studies have focused on diameters greater than 80 mm (approximately 3 inches). In contrast, only a few papers considered pipes with diameters less than 50 mm (2 inches). In the subsequent sections, the types of defects discussed in the literature are reviewed, along with their stages of development and potential causes. After this, the developed NDT&E techniques are discussed.

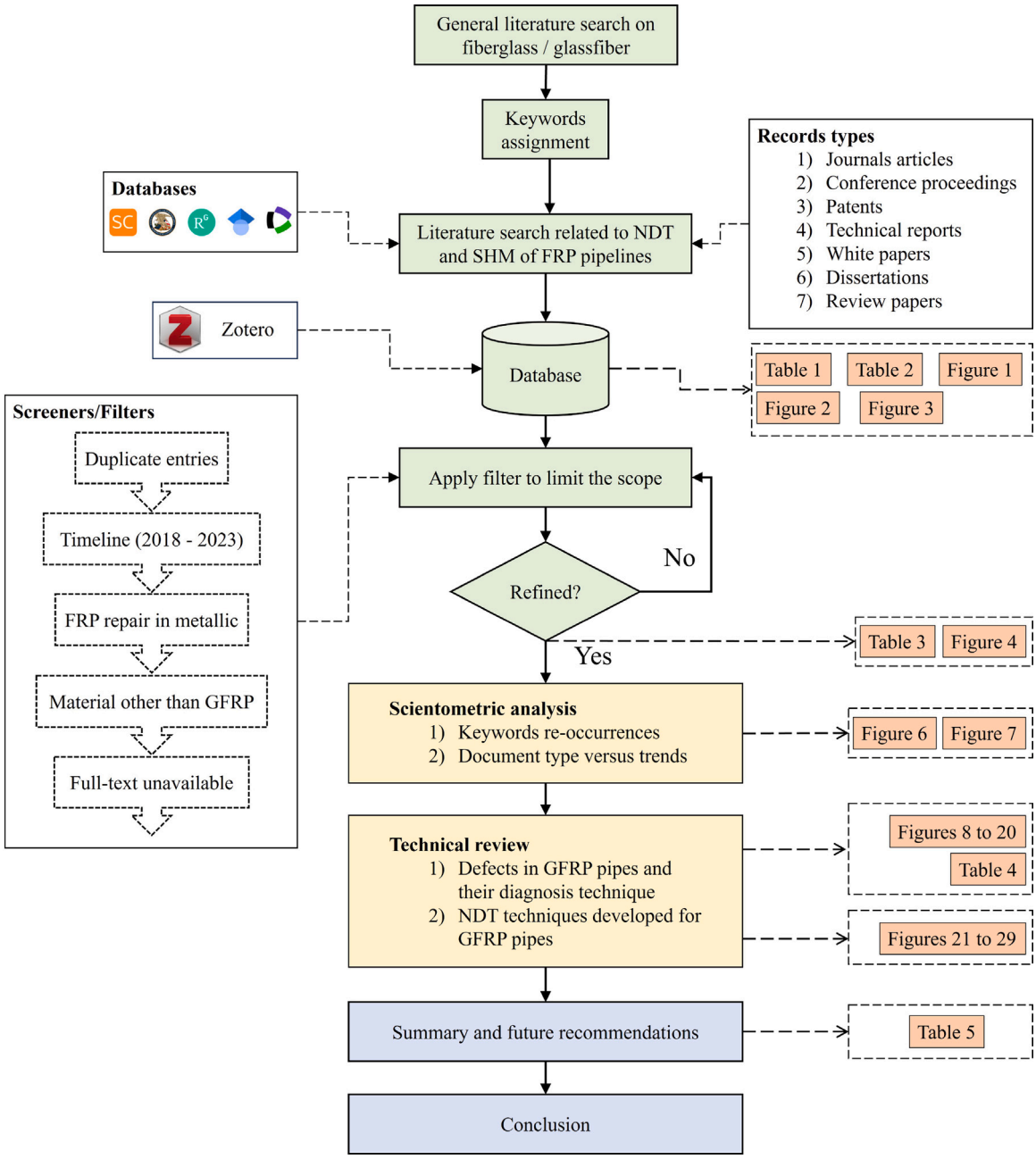

Fig. 5. Workflow and methodology for literature collection, review, and analysis.

4. Defects in FRP pipelines

4.1. General

Despite the numerous attractive properties and advancements in manufacturing techniques, the pipeline industry still has some reservations concerning the widespread use of FRP composite pipes, as reported by many researchers [58–61]. This hesitation stems from several factors, including (i) the long-term performance of composites, (ii) a limited understanding of their failure mechanisms and defect mechanics, and (iii) not having a standard or mature NDT&E techniques for FRP pipelines. The fact that FRP composites pose unique characteristics (e.g., non-isotropic structure, non-homogeneous material, and dynamic mechanical and thermal transient responses [62,63]) which bring complexity in assessing their performance under various environmental and operational

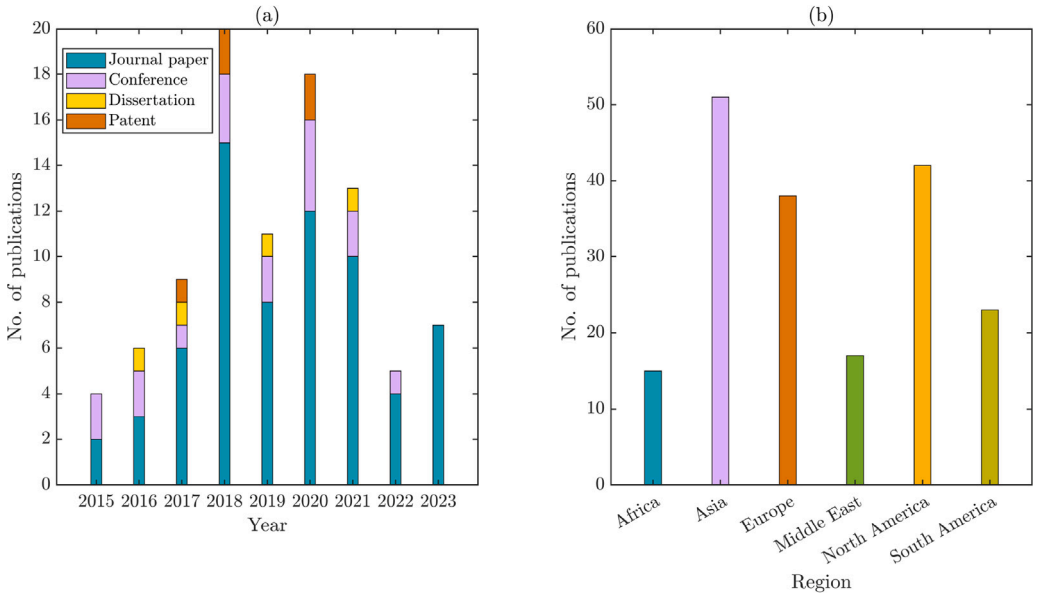

Fig. 6. Number of publications with respect to (a) the document type and publication year, and (b) region of study.

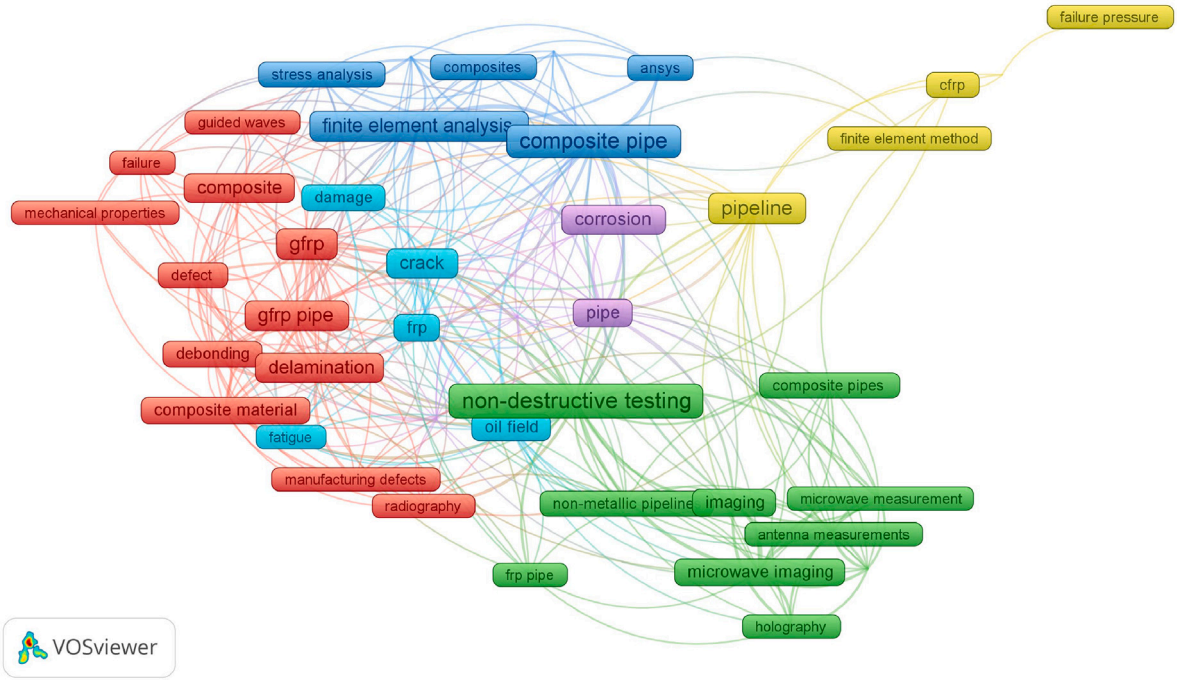

Fig. 7. Keywords re-occurrences map obtained from the literature.

conditions. Additionally, the manufacturing processes involved in casting FRP pipelines are intricate and multi-stage [61,64], further complicating the prediction of their long-term performance.

The limited understanding of failure mechanisms in FRP pipelines is a significant concern [7]. Because of the inherent structural complexity, identifying and comprehending defect progression within FRP pipelines is a challenging task [61,65]. Defects can arise during the manufacturing process [12] or develop over time due to external factors such as harsh environment, sudden or slow velocity impacts, and long-term fatigue [66]. Due to the complex defect mechanics and lack of understanding of the failure root cause, manufacturers/suppliers predominantly rely on visual inspection (following design standards, such as ASTM D2563 [67] or ASTM D3754 [68]) and destructive testing (following standards; examples are provided in Table B.5). Moreover, failure criteria such

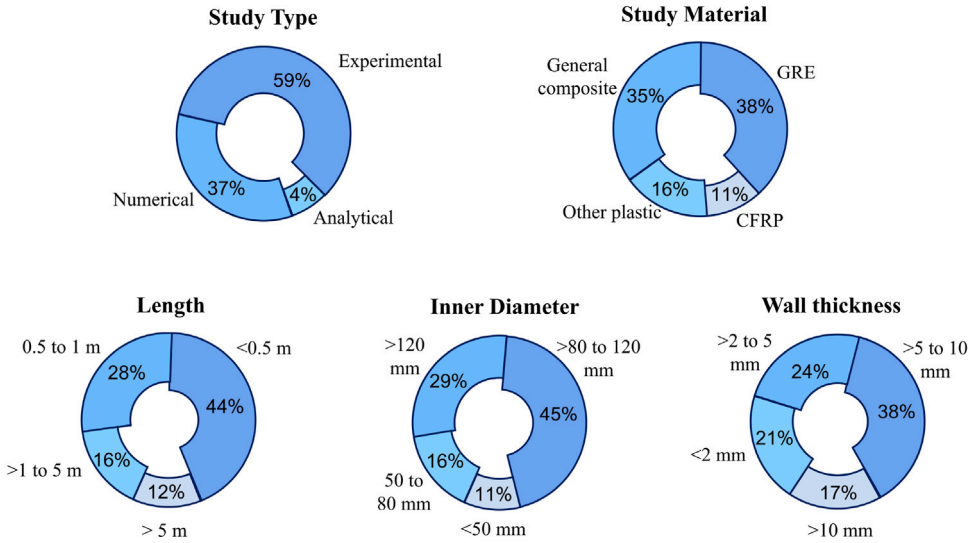

Fig. 8. Summary of the primary characteristics of test pipe specimens used in the literature database.

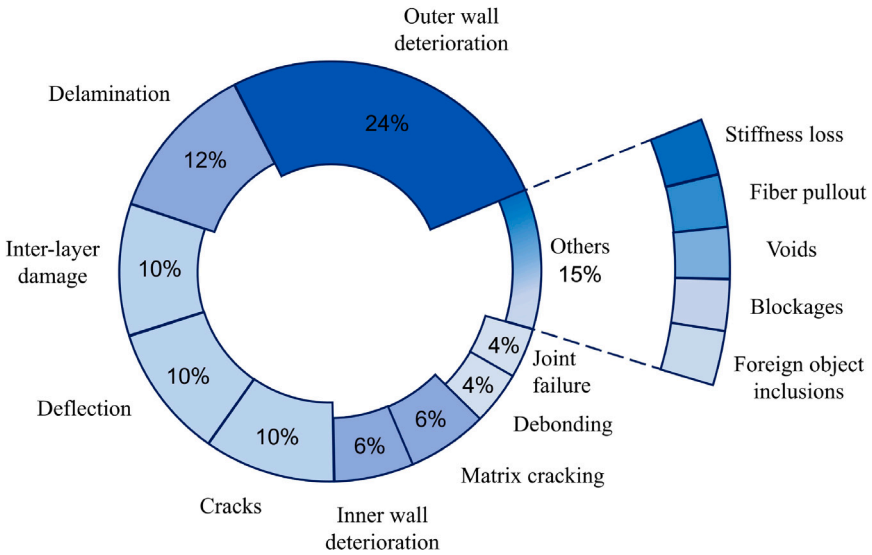

Fig. 9. Summary of different kinds of defects (simulated either numerically or experimentally) discussed in the current literature. The percentages and width of the donuts indicate the frequency of occurrence for each defect type.

as the Tsai–Hill criterion [69] and Hashin criterion [70] remain actively used to predict the onset of composite material failure under complex loading conditions. A comprehensive review of different theories for failure criteria of laminated composites can be found in [71]. Meanwhile, academics and researchers are actively pursuing the development of NDT&E techniques, which have already demonstrated significant potential in diagnosing metallic pipes. In this context, various defect types are studied in the literature. Fig. 9 presents an outlook of different defects simulated numerically or experimentally in the literature database. In what follows, a brief description of each defect type and its stage of development (following [7]) is provided.

4.2. Design and manufacturing stage

4.2.1. General

FRP products (including pipes and fittings) can have defects at both design and manufacturing stages [12]. During the design phase, proper selection of materials, adequate structural analysis, or flawed design decisions can lead to defects in the composite. These design-induced defects can include issues such as reduced load-bearing capacity, weak bonding between layers, or insufficient reinforcement. Likewise, various faults can occur in FRP composites during the manufacturing process. Potter et al. [72] explored

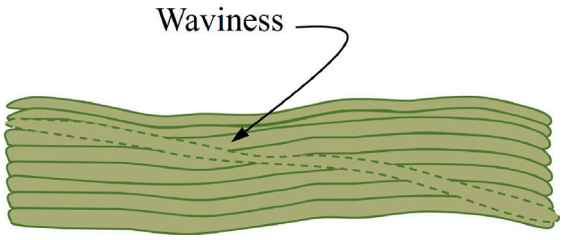

Fig. 10. An illustration of distortion in laminate due to fiber-misalignment.

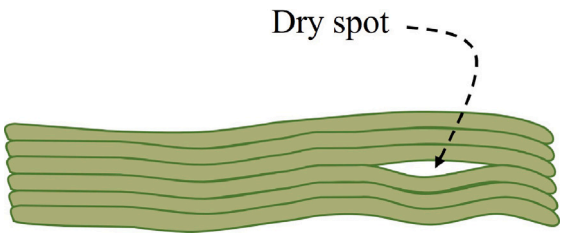

Fig. 11. An illustration of a dry spot due to improper resin penetration.

the influence of fabrication choices on the mechanical properties of composite materials. They emphasized that identifying the composite's structural features at the micro- and mesoscale are essential as they influence the properties of composites. By distinguishing between design-induced "defects" (which can be seen as features) and process-induced defects, they highlighted the need to differentiate between controllable manufacturing conditions and inherent design features. It is also mentioned that identifying actual defect states and variability is crucial, as manufacturing improvements alone cannot eliminate design defects, which must be addressed during the design stage. Common manufacturing-induced defects in FRP pipes are outlined below.

4.2.2. Waviness

Waviness (wrinkling and fiber misalignment) refers to the irregularities or distortions in the fiber alignment within the composite layers. It is a common defect and falls under the category of inter-layer damage (Fig. 9). Fig. 10 illustrates the example of waviness. A real-time fiber misalignment can be found in Figure 2 of [72]. Xie and Zhou [73] highlighted that defects (e.g., cracks or debonding) mostly appear in the direction of the wounded layers. In such a context, the presence of fiber waviness can severely modify the pipe's mechanical performance and structural integrity, as it disrupts the optimal load-bearing capability of the layers. In particular, fiber misalignment can compromise the load transfer efficiency and reduce the stiffness of the material.

4.2.3. Dry spot

The dry spot also belongs to the inter-layer damage category (Fig. 9) and refers to an area within the composite where resin flow has not fully penetrated. Fig. 11 presents an illustration of a dry-spot region. Another example can be found in Figure 1 of [74] wherein the dry-spot was identified in a composite sample that was prepared using the Liquid Composite Molding process [74]. This type of defect can occur due to various reasons such as premature gelling, air trapping during the merging of multiple resin flow fronts, or irregular permeability of the preform. The presence of dry spots, indicating areas with insufficient resin, not only reduces the tensile strength and structural integrity of the composite but also introduces stress concentration points. This combination compromises performance, making the material more vulnerable to cracks, delamination, and potentially leading to premature failure under mechanical loads.

4.2.4. Foreign object inclusion

The presence of foreign materials or particles can inadvertently embed during the manufacturing process. In general, foreign objects may include debris, dust, or other contaminants that are not intended to be part of the composite. Fig. 12 presents an image of a pipe sample wherein a foreign object in the form of Teflon film was intentionally included (during the manufacturing process) to observe the mechanical response of the pipe. In particular, this type of defect disrupts the material continuity and become a potential point of initiation for other defects (e.g., delamination) under stress. It is demonstrated that the presence of foreign object inclusions can compromise the strength and durability of the FRP [61,75], leading to localized weak points or potential areas of stress concentration.

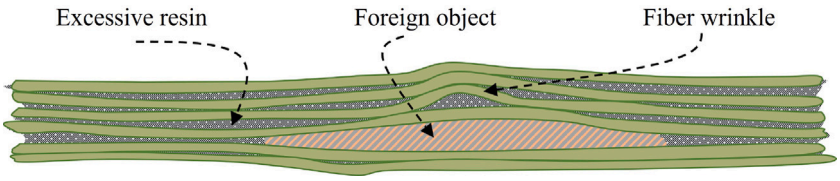

Fig. 12. An illustration of FRP sample with inclusion of foreign object, excessive resin and fiber wrinkling.

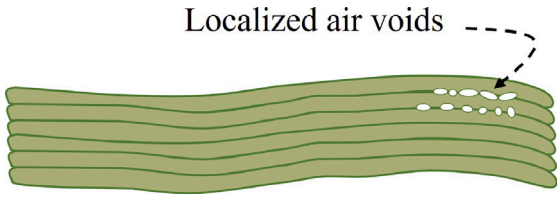

Fig. 13. An illustration of air voids between fiber layers.

4.2.5. Resin lumps

Another common defect that arises during the manufacturing stage is the formation of resin lumps, as illustrated in Fig. 12. These lumps can develop due to several reasons, such as inadequate mixing of resin and hardener or temperature fluctuations. These defects normally appear on the external surface and are detectable through visual inspection. Samples exhibiting lumps are often discarded in accordance with ASTM D2563 standard [67]. Resin lumps create non-uniform stress distribution, compromising the structural integrity of FRP pipes. This can lead to impaired load-bearing capacity, reduced performance, and a heightened risk of premature failure under stress or over time.

4.2.6. Porosity (voids)

Porosity is another commonly occurring defect that refers to the presence of air or voids within the composite material [7,76]. It occurs due to entrapped air bubbles or inadequate resin flow during the manufacturing process [74]. Fig. 13 demonstrates an example of voids in composite material. Porosity-type defects may not cause immediate failure but can result in reduced performance. Over time, and under varying pressure and environmental conditions, these porous areas can become sites of concentrated stress, potentially leading to material degradation, leakage, or structural failure, depending on the application and the severity of the porosity.

4.2.7. Inadequate resin curing

Problems in resin curing occur when the resin does not fully cure or harden during the fabrication stage [7]. It can occur for various reasons, such as insufficient curing time, improper curing temperature, or inaccurate mixing of resin components. Although this defect is not directly addressed (targeted) in the current NDT&E literature collection, it is associated with the category of fiber pullout [77] and/or matrix cracking [78,79] and is equally likely to occur as other fabrication-stage defects. Mechanicall, such types of defect can lead to a sub-optimal polymer matrix, reducing the chemical resistance, and temperature performance.

4.3. Storage and installation stage

4.3.1. General

FRP products generally require special handling and adequate storage [7]. Factors such as exposure to direct sunlight for a prolonged time, harsh weather conditions, or improper stacking can induce stresses in the pipe. They may lead to several defects, including cracks, deflection, shape deformation, etc. Likewise, the transportation of FRP pipes also requires special care and attention. Due to their lightweight (hence small dead load), they are prone to movements during transit. In what follows, several types of defects related to this stage of development are discussed.

4.3.2. Cracks

Cracks are among the top five commonly occurring defects in FRP pipes (Fig. 9), which can arise at various stages, including storage, as well as in-service [12,53,80–82]. They can occur due to multiple factors, such as excessive mechanical stress, improper handling or installation, exposure to harsh environmental conditions, or due to pre-existing manufacturing defects. Fig. 14 illustrates the pipe sample with a crack that appeared on an in-service pipe after six years of operations [79]. Cracks can significantly reduce the fatigue resistance of the composite material and lead to catastrophic failure under cyclic loading.

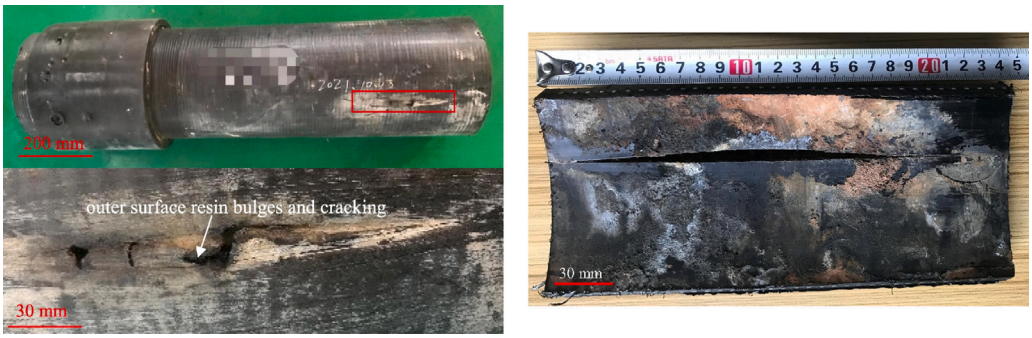

Fig. 14. Steel wire-reinforced composite pipe sample after 6 years of service with a crack [79].

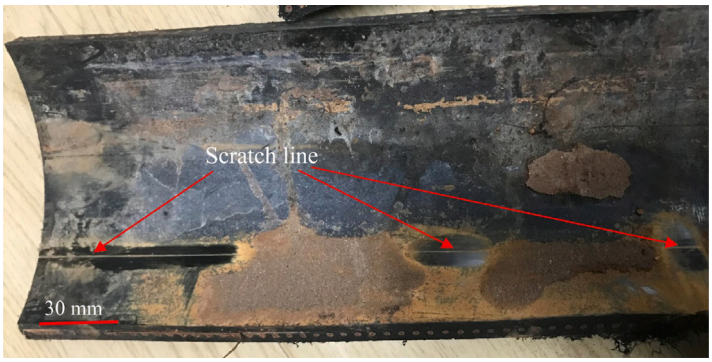

Fig. 15. Example of inner surface wear damage in a 6-year-old in-service steel wire-reinforced composite pipe [79].

4.3.3. *Impact damage*

Impact damage can occur when the pipeline is subjected to sudden or low-velocity (repetitive/continuous) impacts that can induce fractures (see Fig. 17), delamination, fiber breakage, and deformation [73,83–85]. Mechanically, such damage undermines the matrix and fiber integrity, disrupting material uniformity and potentially leading to localized stress concentrations which can significantly impair the overall performance of the pipeline under loading.

4.3.4. *Surface damage*

Surface (interior or exterior) damage has received considerable attention in the literature, constituting 30% of the dataset (Fig. 9). These damages can arise due to several reasons including, but not limited to, continuous rubbing, internal/external abrasion, exposure to harsh environmental conditions such as direct sunlight and heat, and/or frictional forces exerted on the inner surface, all of which contribute to surface degradation [58,60,64,79]. Furthermore, they can lead to material loss and wall thinning [66,86–89], the formation of impact-induced dents [83], the occurrence of surface cracks [12,81], or even the exposure of fibers [7]. Fig. 15 presents a type of internal surface damage found in a 6-year-old in-service composite pipe. Likewise, Fig. 16 shows surface degradation (resin peeling, erosion, pinhole) in a 15-year-old exhumed GRE pipe sample [12].

Surface damage is a particularly alarming as it breaches the protective outer layer of composites. Once compromised, this breach exposes the underlying fibers to environmental elements, increasing the risk of moisture penetration and subsequent degradation of the resin matrix. Such exposure can precipitate a cascade of deleterious effects on the composite's structural integrity, undermining its mechanical strength and durability.

4.4. *In-service stage*

The in-service phase marks a critical period in the lifespan of FRP pipes. In-service pipes play a pivotal role by transporting vital fluids (such as oil, gas, and water), making an uninterrupted supply to fulfill the necessary needs. Given that these pipelines operate under high pressure or even in harsh environmental conditions, the presence of any pre-existing defect or a defect in progression can exacerbate the situation. In other words, any form of disruption caused by defects (e.g., leaks, bursts) during this stage can result in significant repercussions, for instance, paralyzing an entire pipeline network or catastrophic incident in case of oil/gas leakage. Consequently, developing and implementing effective NDT&E for in-service pipes becomes imperative. In this context, several kinds of defects are reported in the literature that belong to this category and are briefly reviewed in the subsequent sections.

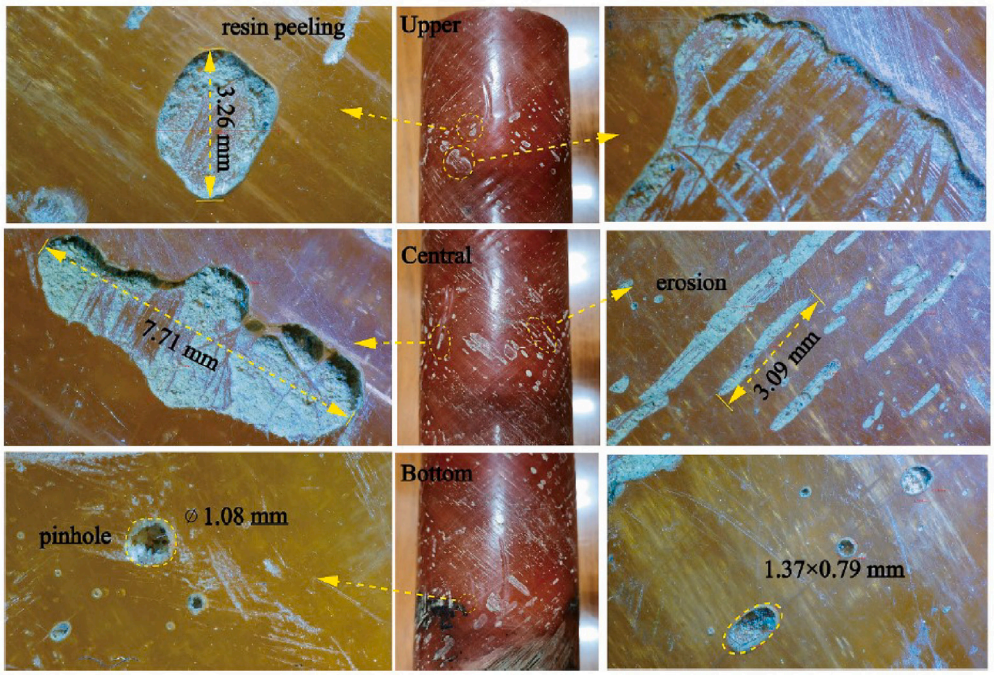

Fig. 16. Example of surface degradation (resin peeling, erosion, pinhole) in a 15-year-old exhumed GRE pipe sample [12].

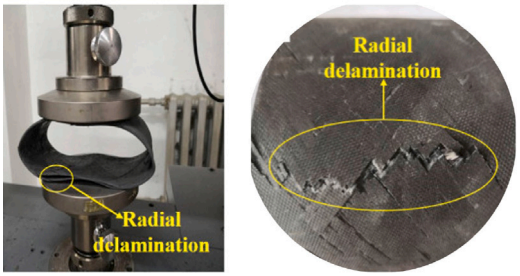

Fig. 17. Example of radial delamination as a consequence of low velocity impact [77].

4.4.1. Delamination

Delamination ranks as the second most commonly considered defect in the literature (Fig. 9) in reference to the in-service stage [61,66,77,81,85,90,91]. It refers to the debonding/separation/detachment of layers or plies within the composite material. As the name implies, delamination occurs when the bond between adjacent fiber layers weakens or fails due to pre-existing manufacturing/storage defects, excessive stresses, prolonged in-situ low-velocity impact, or any combination of the above. It is a critical defect that can compromise the pipe's structural integrity, reducing its strength and potentially leading to premature failure, bursts, and/or leakage [66]. Fig. 17 shows an example of radial delamination as a consequence of low-velocity impact [77].

4.4.2. Leakages

Leaks are often rooted in underlying defects, such as wear damage, dents, inter-layer delamination, and/or debonding. These defects, when coupled with intensive operational conditions or requirements, have the potential to exacerbate and propagate, eventually leading to leakages. In literature, several publications have considered leakages [53,88,92–95]. A leaking pipe not only compromises the structural integrity of the system but also contributes in non-revenue losses, as substances like oil, gas, treated water, or sewage leak to the environment. To give a perspective, leaks are responsible for 32 billion cubic meters of freshwater water loss per year worldwide [96].

4.4.3. Pitting

Albeit less relevant to FRP, pitting in steel-reinforced composite pipes is a common problem reported in the literature [79,84]. It refers to the localized corrosion or degradation of the steel reinforcement, resulting in small, localized pits or cavities. Fig. 18 shows

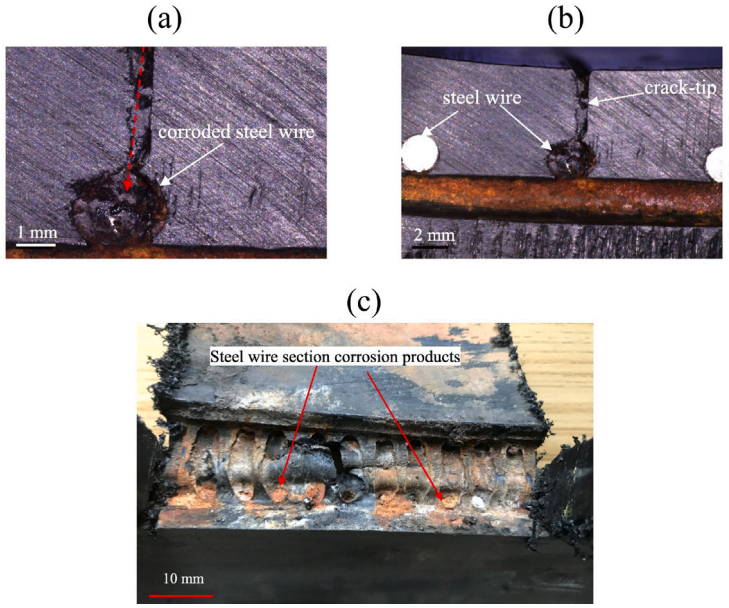

Fig. 18. Example of pitting corrosion in a steel wire-reinforced composite pipe sample reported in [79].

Fig. 19. Example of a blocked pipe due to depositions.

an example of pitting corrosion in a steel wire-reinforced composite pipe sample. It can lead to reduced wall thickness, weakening of the pipe structure, and potential leakage or premature failure.

4.4.4. Chalking

Chalking presents a distinctive trait within composite materials. It is observed as a powdery or chalky residue on the surface, resulting from the degradation or deterioration of inter-layers within the pipe. This phenomenon often signifies the advancement of aggressive defects such as cracks, surface deterioration, or sudden impact, indicating an impending issue, and has been reported by many authors [12,53,81,92]. A chalked surface implies that the representative pipe surface has initiated degradation, weakening the protective barrier of the FRP pipe and rendering it susceptible to additional damage, including cracking and erosion.

4.4.5. Other material-related defects

Several other defects are also considered by a few papers, including (i) blockages [26], (ii) blistering [66], and (iii) permanent deflections [97]. Blockages, arising from a variety of physical and chemical processes such as material deposition and plaque accumulation (see Fig. 19(a)), contribute to increased energy consumption, leading to both energy and financial losses. Blistering, on the other hand, is typically formed due to inter-layer debonding or the presence of voids (see Figure 1(c) in [66]), resulting in raised or swollen surfaces that compromise the structural integrity of the pipe. In contrast, permanent deflections in fiberglass pipes occur due to prolonged loading or excessive external forces, resulting in the pipe's original shape deformation.

Fig. 20. Example of pipe burst subjected to quasi-static internal pressure with an external lateral dent in an RTP pipe [83].

4.5. In-service piping system failures

While most of the defects mentioned above are either simulated in a controlled environment or observed in a non-functional pipe, some studies have also reported failures of FRP piping systems during their in-service and operational stages. Piping systems are intricate, comprising extensive pipelines with varied topologies, dynamic mechanical devices (e.g., pumps and valves), and many hydraulic appurtenances (e.g., bends, junctions, and flow controllers). Malfunctions in any of these components, such as valve jamming/slamming or excessive pump vibrations, can lead to severe problems. Intense operational activities can adversely affect an internally defected or even defect-free pipe system, resulting in service downtimes, outages, increased repairs, rehabilitation, and maintenance costs. In this context, several studies have documented issues with in-service fiberglass piping systems. For instance, [83] highlighted an in-service and internally pressurized pipe burst due to an external dent in the lateral direction, as illustrated in Fig. 20.

Similarly, Liao et al. [12] documented the failure of a 15-year-old GFRP pipeline used in a sour oilfield, attributed to cavity defects caused by insufficient air bubbles and resin filling. Petrobras, a leading Brazilian multinational petroleum corporation, indicated that nearly 90% of failures in their FRP pipelines result from improper installation [25]. This underscores the importance of regular inspections and condition assessments of FRP pipes throughout their lifecycle, spanning from delivery and installation to in-service operations. Additionally, Guoquan et al. [53] reported leakage in a recently installed GRE pipe in an oil field caused by numerous circumferential cracks on its external wall. Another study, [79], presented a case of a severe burst in a steel wire-reinforced thermoplastic composite pipe, which occurred a few months after its installation, pointing to environmental stress cracking (ESC) of its base resin as the cause. In a related account, Saad et al. [83] described a sudden rupture in an in-service GRP elbow used in a cooling water system. This failure was deemed premature since the elbow's design life was 25 years, but the rupture took place in just seven years of its service.

5. Non-destructive testing techniques for FRP pipes

5.1. General

In this section, emphasis is made on several NDT&E techniques that have been developed and tested on FRP pipes or piping systems. For each method, a brief introduction is first provided. Then, the contributions from different researchers are reported. For illustrative purposes, a buried pipe configuration is used as a standard theme to demonstrate and compare NDT&E techniques in terms of their operational requirements/settings.

5.2. Visual inspection (VI)

Visual inspection is one of the simplest and most practiced techniques for NDE of pipelines. It is less expensive, quick, and sometimes informative enough to provide sufficient information for decision-making, eliminating the need for additional advanced NDT&E methods. This class of inspection is suitable for on-site inspection during manufacturing installation, as well as for in-service and accessible pipelines, and is commonly adopted to diagnose any visually apparent macro-scale defect such as surface cracks, misaligned joints, leakages, etc. A VI may also include hand-held devices such as cameras, flashlights, endoscopes, UAVs for elevated piping systems (generally used in buildings), and glass magnifiers.

Among various forms of VI surveys, the liquid dye penetration inspection is also a common NDT method for inspecting external macro-scale defects. It is a contact-based technique that requires access to the pipeline itself, and it is only suitable for external

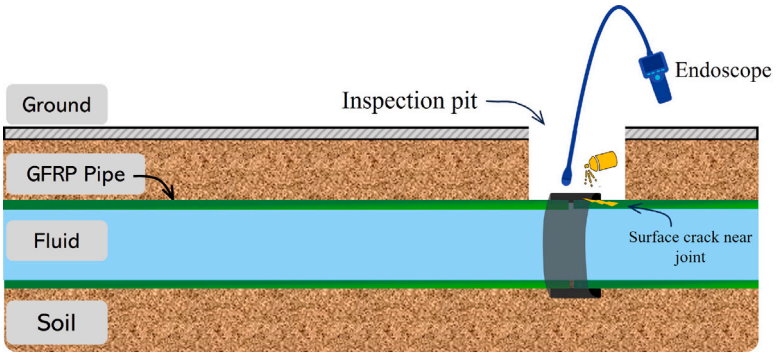

Fig. 21. Illustrative example of visual inspection for a buried pipe. An initial estimate of the defect along with an inspection pit is needed for inspection in case of underground pipelines.

defects such as cracks and porosity. The methodology involves site preparation (such as the surface provision of an inspection pit, target surface cleaning, etc.), followed by the application of a liquid dye (or paint spray) on the target pipe surface, followed by a wiping process to unveil the surface-breaking defects that are large enough to be observed with the naked eye or using the endoscope, as demonstrated in Fig. 21.

In literature, most of the papers have performed VI on mechanically stressed pipe samples. Ren et al. [77] conducted a numerical study and simulated several types of defects such as delamination, fiber pull out, debonding, holes, and cutouts in the presence of mechanical loading in radial and axial directions. Their study noticed the shape recovery after radial compression with reduced strength. In contrast, axial compression induced mid-length buckling and delamination in the samples. Since this study was conducted numerically, VI inspection was conducted virtually based on deformation and stress graphs.

Leon et al. [62] conducted an in-depth analysis of GFRP laminates covered with HDPE. Their method employed an open-hand lay-up technique with 0- and 90-degree orientations. Their study involved both tensile and compression tests following ASTM standards D3039 and D6641, respectively. Additionally, ANSYS software was utilized to perform numerical validation of their results. The specimens underwent mechanical loading in various forms, including tensile and compression in both axial and radial directions, as well as shear in the YZ plane. The process continued up to the point of bursting. In this study, the axial stress concentration was closely monitored using the UMT Bionix tensile machine. Three boundary conditions were taken into account, specifically open-end, fixed-end, and closed-end. This study performed VI manually and reported a non-uniform stress distribution across the specimens.

In another comprehensive study by Shi et al. [61], the focus was on glass fiber tape reinforced pipe samples constructed from 12 plies (oriented at ±55–degree angles). The pipe samples were filled with water and then internally pressurized in accordance with ISO-1167. For numerical assessments, the ABAQUS software was employed, supplemented with a subroutine on UMAT. The testing methodology was primarily hydro-static, with samples being pressurized until they burst. Specific tests on delamination, with lengths ranging from 50 to 150 mm, were also performed up to the point of rupture. To introduce delamination-like defects, Teflon film around the entire circumference and between the 6th and 7th layers was intentionally added during manufacturing. This research highlighted that during the manufacturing phase, delamination is almost an inevitable occurrence, leading to local stress concentration regions and becoming precursors to premature defects. The authors performed manual VI and observed that the presence of delamination contributed to a decrease in the burst pressure. Additionally, different failure morphologies were noticed based on the extent of delamination. Interestingly, the authors found a correlation between these failure morphologies and the width of the glass fiber tape. This correlation presents a promising avenue for further research.

In a similar regard, Elhady et al. [66] undertook a comprehensive examination of a 30-year-old seawater handling GFRP pipe. This study was primarily focusing on detecting the critical osmotic blister. For this purpose, the authors modeled osmotic blisters as surface notches of various sizes. To gauge the longitudinal pipe strength, they employed tensile testing methods using a Universal Testing Machine (Instron 8801, UK). Additionally, for numerical evaluations, they utilized ABAQUS software and the Hashin Criteria [70]. They utilized an empirical approach to determine the critical notch size beyond which the material's tensile strength is significantly compromised. It is observed that osmotic blisters frequently appear on the external surface of GFRP pipes. These blisters, although common, are usually disregarded in many evaluations. The authors also found that if a surface notch has a depth equal to that of one layer, it does not significantly impact the longitudinal strength of the material. Another paramount insight from this study was the role of delamination between the layers. It was deduced that such delamination plays a pivotal role in determining the ultimate strength of the material.

In another study conducted by Abu Bakar et al. [83], reinforced thermoplastic pipes (RTP) equipped with an internal liner and an outer cover were examined. The authors conducted a burst test in accordance with ASTM D1599. The primary objective was to evaluate the pipe's resistance to pressure leading up to rupture, especially when the pipe has a dent, designed to replicate the damage from an anchor drop. Their paper mentioned that the effects of such external and sudden impact loading generally lead to two types of discernible defects: (a) a single unit failure, characterized by a sudden and immediate rupture, and (b) a ply-by-ply failure, which entails a more sequential and gradual breakdown of the material. Building on their findings, the authors proposed

an empirical formula that allows for the estimation of a pipe's burst capacity by accounting for the properties of the dent and the associated lateral loads.

In Liao et al. [12], the focus was made on fiberglass (E-class) pipes, constructed explicitly with 11 layers, each featuring a ±45-degree spiral winding. Their research centered on understanding the effects of a 10 cm long and 3.5 cm wide crack that ran parallel to the direction of the fiber winding on the ultimate strength of the pipe. Their findings revealed uneven resin distribution in the pipe samples, along with clear indications of spalling, peeling, linear scour marks, and the existence of pinholes. Notably, even though they observed external resin peeling, the authors did not conclusively attribute it as the immediate cause of the pipe rupture.

Qi et al. [53] conducted a comprehensive study on E-glass GRE pipes. They employed several techniques such as Differential Scanning Calorimeter, Muffle Furnace, and Analytical Balance for their investigations. The computational analysis was done using ABAQUS. Their tests included both bending and hydraulic pressure assessments. A significant observation from their study was a leakage failure located 40 cm away from the threaded end of the pipe. This was particularly notable in a GRE pipe sample exhumed from an oil field that experienced this leakage during a post-installation pressure test. The authors found that bending stress applied externally instigated circumferential cracks on the pipe's exterior, subsequently diminishing its capacity to bear internal pressure. Further visual inspection highlighted fiber whitening, oriented in the winding direction, close to the site of the leakage.

In another comprehensive study undertaken by Sulu and Temiz [92], the authors examined samples of E-glass GRE pipes consisting of 4 layers. The ply-angle in these layers varied between ±55-degree and ±30-degree. For testing, they referred to several ASTM standards, such as D3039-76 for tensile testing, S3410 for pressure testing, and D7078 for shear testing. The computational analysis was achieved using ANSYS (SOLID 186 element). The pipes were internally pressurized until a sleeve failure was noted. They employed the Tsai Wu failure criteria [69] to evaluate pipe failure and the Von-Mises failure criteria [98] for the adhesive component. The main objective of their research was to analyze the failure mechanisms of internally pressurized GRE sleeves. Through experiments, they captured and documented radial, tangential, axial, and shear stresses across the thickness direction. In parallel, they numerically determined the Von–Mises stress distribution within the adhesive component. A distinct "whitening effect" (as described earlier in Section 4.4.4) was observed during and in the proximate to the rupture phase. A significant conclusion from their work was the identification of sleeve length and adhesive type as primary determinants of joint strength in such configurations.

Samanaci et al. [81] explored the dynamic behavior of E-glass GRE pipe samples, constructed explicitly with a winding of layers patterned as $[\pm 75]_3$. They employed strain gauges in both axial and radial directions to capture detailed measurements and conducted a hoop stress test (following ASTM D2992). The pipes under examination were internally pressurized using hydraulic oil, operating at a frequency of 0.42 Hz. The pipe samples were machined to bear semi-elliptical surface cracks. The primary focus of their research was to understand the dynamic response of these delaminated areas with respect to fatigue cycles.

In a detailed study by Saad et al. [82], the authors meticulously examined the structural integrity of GFRP 90-degree mitered bends through VI and mechanical testing. The authors employed an Instron 250 kN testing machine to conduct tensile and compression tests at a strain rate of 0.01/min. Additionally, SolidWorks was utilized for design purposes, and computational evaluations were performed using CFD and FEA methods in ANSYS Workbench. A significant insight from their study was the identification of bend rupture due to a subpar fabrication process. Their examination revealed that the immature rupture of the in-service GFRP bend was primarily due to flaws in the fabrication process. Consequently, they advised against using a 45-degree fiber orientation for such applications. Visual analyses of the bends further highlighted that most cracks were dry and brittle, signifying a compromised fiber–matrix interface. Furthermore, an internal ridge, indicative of fabrication inconsistencies, was discerned. While the pipe was wounded with 45-degree fibers and later subjected to mechanical tests, anomalies were visually observed. The stress–strain curves displayed "knees", hinting at the presence of micro-cracks within the matrix. Finally, variations in thickness were identified, which led to non-uniform stress distributions and the formation of multiple internal ridges.

In summary, VI is frequently and dominantly used in the literature due to its ease of practice and robustness. Moreover, this technique is found to be efficient and effective in diagnosing observable/apparent problems, thus minimizing the efforts needed to use extensive and much more involving NDT&E techniques. Many insights were unveiled in the literature, attesting to the efficiency of this approach. However, the limitations of VI remain prevalent. While it can offer detailed insights into existing defects and structural behaviors, its reactive nature means it can detect issues only after they have manifested. Furthermore, VI is labor-intensive, time-consuming, and inefficient in diagnosing early-stage or subsurface anomalies that do not present overt visual cues. In the context of buried pipes, VI necessitates the construction of inspection pits, which are excavation areas enabling close examination of the pipe's exterior within a localized scope. Moreover, this method is limited to the specific location around the pit, leaving the rest of the pipeline uninspected. It also fails to detect internal issues such as corrosion and blockages. In addition, due to the cost and practical constraints of creating inspection pits, only a fraction of the pipeline can be visually assessed. Consequently, while VI is invaluable for comprehensive post-issue diagnostics, it underscores the need for complementary predictive and proactive NDT&E techniques to ensure holistic pipeline health assessment.

5.3. Guided waves ultrasonic testing (GWUT)

Guided waves ultrasonic testing is a popular contact/non-contact-based active sensing technique that has received immense attention for metallic pipeline health assessment and defect detection. This technique is based upon high-frequency[1] elastic/mechanical/stress waves that are intentionally induced within the pipe wall. These waves propagate along the pipe in

[1] The term "high-frequency" is used when the wavelength of the injected waves is comparable to the shortest pipe dimension in the interested direction of the pipe (e.g., pipe radius in the case of longitudinal/radial wave modes or pipe wall thickness in the case of lamb wave modes). At such a length scale, the injected waves are also expected to disperse, providing a connection with the concepts of group and phase velocities.

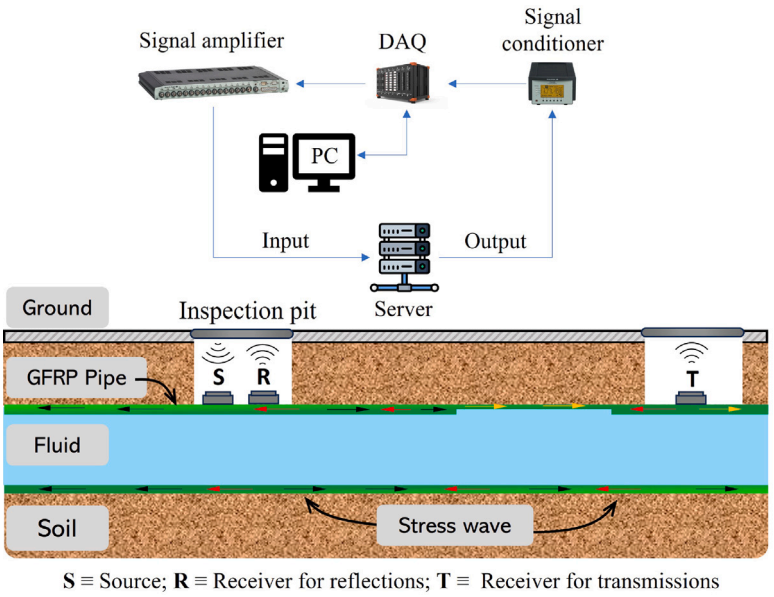

Fig. 22. Illustrative example of the guided waves ultrasonic technique. It involves an active wave source (**S**) which receives the signals from the operator and injects stress waves by means of local vibrations into the pipe walls. These waves are guided by the pipe wall and propagate in axial, radial and circumferential direction, depending on the dispersion behavior of the pipe and injected frequency bandwidth. The receiver can be configured in a (i) pitch-echo mode where receiver (**R**) would receive reflections from the abnormalities, or (ii) pitch-catch mode wherein receiver (**T**) would receive the transmitted waves.

longitudinal and circumferential directions and reflect part of the energy whenever they encounter a change in the impedance of the pipe due to known physical boundaries or unknown and invisible defects in the pipe wall.

The methodology of GWUT on a buried pipeline system is illustrated in Fig. 22. The setup typically comprises a pair of transmitters (e.g., EMAT or piezoresistive sensor/transducer), a receiver (piezoelectric transducer/accelerometer), data acquisition devices, signal conditioner, an amplifier, and a PC for inspection and visualization. The steps for performing GWUT involve an injection of a user-defined analog signal (voltage or current) in the form of a Gaussian-modulated sine or a toneburst from the PC to the data acquisition (DAQ) device. An illustration of the preceding waveforms is provided in Fig. 23. The DAQ translates the analog signals into electrical signals and passes them to the amplifier for amplitude amplification. The amplified signal is then transferred to the transmitter. The transmitter converts the received electrical signals into mechanical signals and induces strains at the place where it is attached. The mechanical vibrations caused by the local displacement propagate concentrically (depending on the directivity pattern of the transmitter). The receiver, on the other hand, senses the local vibrations in the form of wave packets (arriving at different times, depending on the material properties) and transfers the signal to the conditioner for filtering the obtained signal from environmental/electrical noise. Then, the signals are transmitted to the PC through DAQ for visualization and analysis.

In general, there are two ways to configure the pair of sensors: (i) pulse-echo configuration and (ii) pitch-catch configuration. In the former, the receivers are placed adjacent to the transmitters. The target is to record the reflections induced by the defect(s) or known/unknown physical boundaries in the form of echoes. In the latter configuration, on the other hand, the receiver is placed at a known distance away from the transmitter to record the transmitted waves. Both reflected and transmitted signals contain encoded information regarding the defect size, location, number of defects, and shape. The recorded signals are then used in conjunction with numerical/analytical models, replicating the actual test specimen, to discern the defect location/type/size and health status of the system.

Before exploring the literature review on GWUT, it is worthwhile to explore the dispersion characteristics of high-frequency ultrasonic guided waves. Ultrasonic waves exhibit dispersion behavior in the sense that when a bandwidth of a signal is injected into the system, the initial wave packet disperses in time. This dispersion leads to waves of different frequencies propagating at different speeds, which is known as the phase speed and defined in Eq. (1) as

$$c_p = \frac{\omega}{k} \tag{1}$$

where c_p denotes the wave speed (in m/s), k represents wavenumber (in 1/m), and ω is the angular frequency (in rad/s). While each frequency picks up its own speed, the energy of the injected signal propagates with the group velocity, denoted by c_g and defined in Eq. (2) as

$$c_g = \frac{d\omega}{dk} \tag{2}$$

where d represents the first derivative. The group velocity can also be expressed in terms of phase velocity, given in Eq. (3), as

$$c_g = c_p - \lambda \frac{dc_p}{d\lambda} \tag{3}$$

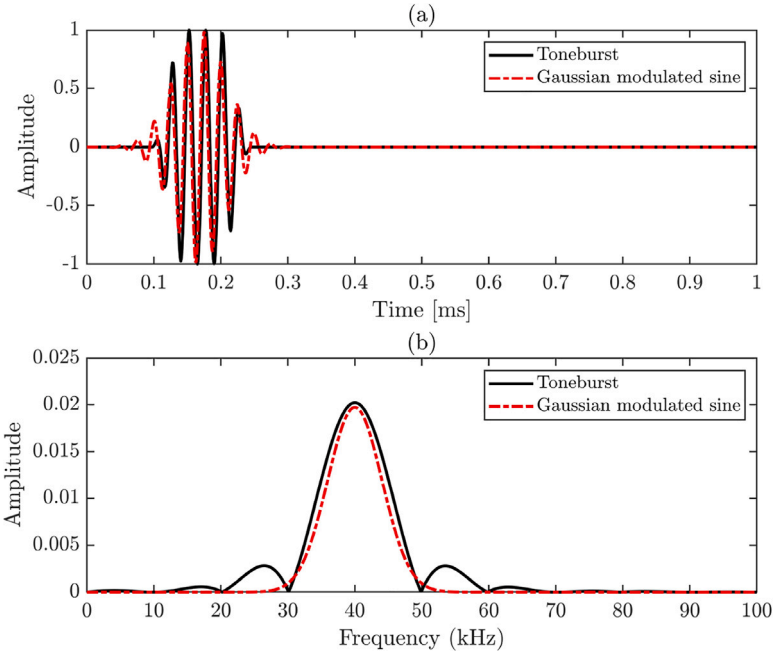

Fig. 23. Example of toneburst (solid line) and Gaussian modulated sine (dash-dot line) in (a) time and (b) frequency domains. The signals are generated with the sampling frequency of 1 MHz, and central frequency of 40 kHz. The total time length of the signals is 1 ms and the signals bandwidth is defined as $[0.9, 1.1] \times F_c$, where F_c is the central frequency.

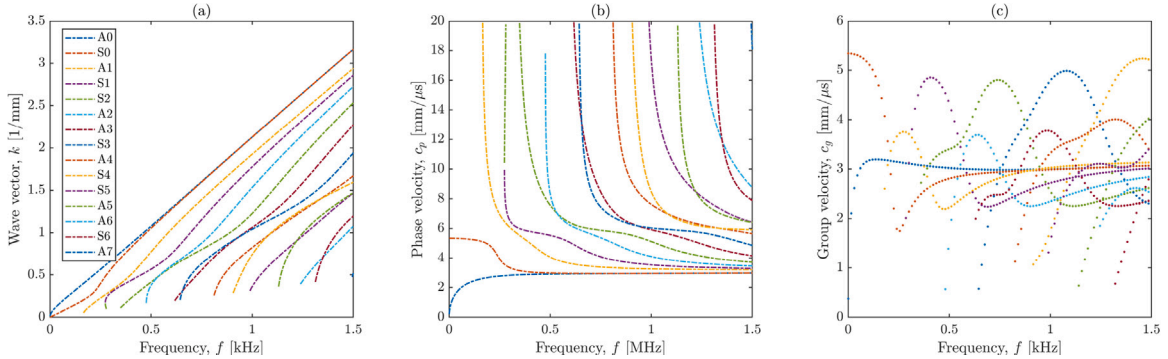

Fig. 24. Lamb wave modes (dispersion curves) of a 10 mm thick pipe wall. (a) wavenumber versus frequency plot, (b) phase speed versus frequency plot, (c) group velocity versus frequency plot. In legend, "A" and "S" denote asymmetric and symmetric modes.

wherein λ is the wavelength. Note that while ω is user-defined, k is usually governed by the material properties and waveguide geometry. As such, understanding the dispersion properties of guided waves contributes to understanding wave-defect and wave–structure interactions. Fig. 24 presents an example of a dispersion curve (Lamb wave modes) for a 12-inch diameter pipe with a 10 mm wall thickness. In this figure, each line is called "mode", whose propagation speed is frequency and material properties dependent. In most physical problems, $c_p > c_g$, implying that the signal envelop expands in the time domain. This is because some waves travel slower than others. For the case where $c_g = c_p$, the propagation is non-dispersive as in plane wave propagation. For $c_p < c_g$, the behavior is called "anomalous dispersion" which occurs in specific materials or under certain conditions. For detailed understanding of Guided waves, encompassing their distinct types (including Lamb, Shear, Torsional, Flexural, and Rayleigh waves) and the modeling techniques, readers are encouraged to refer to seminal works such as those authored by Rose [99], Achenbach [100], and Kundu [101]. These references offer comprehensive insights into the diverse characteristics and techniques associated with GWUT.

In the literature database, four articles were found that are relevant to the scope of this paper. In what follows, the scientific contributions of these papers are summarized. Gresil et al. [58] examined a composite pipe made of 5 alternating layers of uni-directional carbon fiber (T700) and glass fiber (E-class). They employed piezoelectric wafer active sensors (PWAS) positioned upstream at the pipe crown for signal emission and mid-length and downstream for reception. With an input signal of 80 V, featuring

a three-peak toneburst within a 15 to 750 kHz range, they utilized ABAQUS and ANSYS for numerical simulations and validation, respectively. Their research primarily focused on various elastic wave modes, both longitudinal modes (L(0,1), L(0,2), L(0,3)) and torsional modes (T(0,1) and T(0,2)). Their investigation involved assessing an artificial defect represented by a gel-coupled coin. Their findings highlighted the use of PWAS to excite longitudinal modes and a noted decrease in damage index with increasing frequency. Interestingly, no torsional mode was detected in their experiments. Moreover, they emphasized the need for baseline data from pristine pipe samples to discern the defect signatures in the measured responses.

In another paper by Carrino et al. [60], the authors shifted their focus to a composite pipe (made by filament winding of pre-preg glass fiber in 4 layers). They utilized an array of five piezoelectric transducers (PZTs), with one at the crown for signal transmission and four others positioned along half the pipe's circumference for reception. A voltage signal characterized by a five-peak toneburst ranging from 50 to 200 kHz was used. They also utilized ANSYS for numerical simulations wherein Lamb wave modes, specifically S0 and A0, were excited. For defect simulation, they also used a 1 Euro coin, artificially coupled on the exterior side with a thermoplastic adhesive. Among their significant findings, Carrino and his team used pitch-catch data in axial and circumferential dimensions to analyze lamb wave propagation. They accurately determined the helical path length and the corresponding propagation angle. An essential aspect of their methodology was its ability to operate without a baseline. They also highlighted that when the radius is greater than 10 times the thickness, the curved plate behaves similarly to a flat one. However, they noted that their PWAS setup could not excite SH modes. Moreover, they introduced a probability density function that permitted the mapping of Time-of-Flight (ToF) data onto a defined space while adhering to geometrical constraints.

Joas et al. [64] embarked on a study involving CFRP pipes, choosing to employ air-coupled ultrasound, specifically utilizing non-focused ultrasound probes AS200T from Air Star Inc. The specifics regarding the experimental setup remained largely unspecified. Their focus was directed towards the Slanted re-emission mode (SRM). The nature of the defect they aimed to detect involved outer wall deterioration, artificially simulated using rectangular patches of adhesive tape. Joas's team employed a unique approach, conducting A-scans in the circumferential direction with the help of air-coupled ultrasound equipment. Notably, they integrated a robot to facilitate the movement of the transducers in the axial direction. They accurately determined the axial positions of the defects; however, the circumferential locations remained elusive.

Almeida et al. [91] conducted their investigations on GRE pipes that were manufactured using filament winding at an angle of ±55 degrees. For their studies, they employed a 32-element matrix probe operating at a frequency of 500 kHz. They used 0.1 mm thick acetate sheets between the fiber plies to simulate inter-ply delamination-like defects. In total, six flaws of variable dimensions were created. Their primary methodology entailed using an ultrasonic (UT) phased array to detect delamination in GFRP laminated joints, which were joined using the hand-lay process. These joints consisted of a composition of 7 glass fiber layers, two woven rovings, and five mats, all impregnated with epoxy resin. The samples were submerged underwater for scanning to ensure comprehensive coverage and gain the SNR. Their findings were insightful, wherein they detected 5 out of the 6 intended defects. Additionally, their process brought to light other unexpected flaws in both their controlled and intentionally flawed samples. These findings were further verified through Computed Tomography (CT) scans.

Based on the foregoing review, it is evident that GWUT has found applications across various composite pipes. Both bulk and guided wave modes have been studied to understand their nuances. Notably, Carrino et al. [60] displayed profound insights into Lamb wave propagation characteristics, deriving essential parameters like the helical wave path length and propagation angle. Various defects have been investigated, ranging from surface deterioration exemplified by coupled coins to intricate issues like delamination and fabricated joints.

In the context of buried pipes, GWUT requires an inspection pit to install transducers. However, once the transducers are positioned, GWUT can theoretically inspect the neighboring buried section up to a specific length. This length depends on the input signal's strength, background noise, damping factors, and dispersion properties of the medium. While significant efforts have been made in exploring modes such as the longitudinal and Lamb waves, some areas remain unexplored. For instance, torsional modes largely remain unexplored in existing studies, indicating room for further investigation. Another evident challenge lies in the need for baseline data and pristine conditions, often unavailable in practical scenarios.

Additionally, there is a pressing need to pay attention to wave-defect interactions. This will elucidate how a specific wave mode interacts with certain defects and how this interaction modifies the overall waveform of the measured signal. Sensitivity analysis, based on frequency bandwidth, also warrants further exploration. In the realm of technological innovation, integrating machine learning or artificial intelligence offers promising avenues, especially in automating and improving defect detection in composite materials. To summarize, the field of guided wave methodology for NDT of composite pipes has yet to see any remarkable progress. However, there are still untapped potentials and prevailing challenges. These represent invaluable opportunities for future research and technological breakthroughs.

5.4. Acoustic emission techniques (AET)

The acoustic emission technique is a contact-based passive sensing technique which relies on detecting the transient stress/elastic/mechanical waves in the pipe wall. These waves are generated in response to the energy released by progression in defects such as matrix cracking/debonding, local delamination, fiber pullout, etc., due to external/internal impact. This impact could be intentional, such as a sudden change in temperature and pressure, or unintentional, such as low-velocity impact due to external sources such as ground motion (e.g., earthquake), long-term exposure to mechanical vibrations and/or cyclic traffic loading, in case of a buried pipe system.

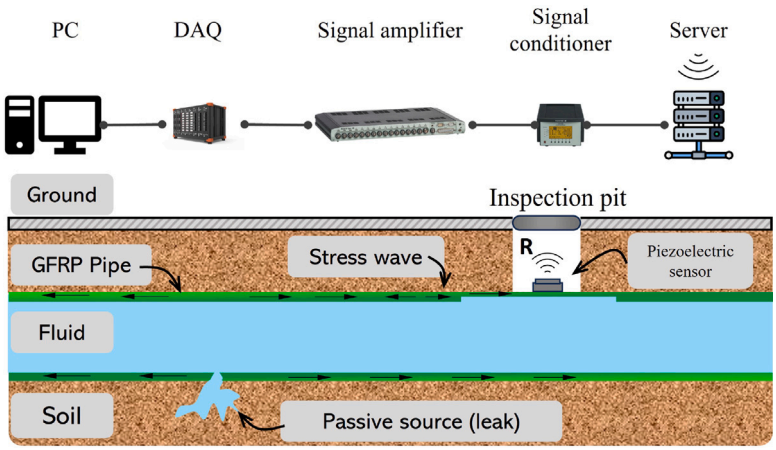

Fig. 25. Illustrative example of the acoustic emission technique. It involves passive sensing of stress waves that are being generated by the defect in reaction to external sources (e.g., low-velocity impact, high internal pressure, etc.). The defect-induced waves are recorded via receivers (**R**) and transmitted to the server either wirelessly or via wired connections.

The application of AET for the case of a buried pipeline system is illustrated in Fig. 25. The standard procedure and testing protocols to perform AET on composite pipelines are outlined in ASTM E1118 [102]. In essence, this technique requires an array of sensors (e.g., piezoelectric transducers/accelerometers), which are sensitive to small strains/displacements, a data acquisition device to operate the sensors, and a transmission device to transfer the data to a nearby control station through a wireless or wired connection. The control station receives the signal and applies the user-defined filter(s) (to suppress the noise) and an amplifier to magnify the recorded signals. The recorded signals are then processed using wave analysis algorithms. In essence, these algorithms are developed on the principle of time-domain reflectometry whereby the arrival time (time-of-flight) of the wave is translated into the distance using the group velocity information. The group velocity refers to the speed at which the wave packet (a group of waves instead of individual wave modes) propagates inside the medium. A simplified form of calculating the defect location using the time-of-flight information is defined in Eq. (4) as

$$x_d = c_g \frac{t_f}{2} \tag{4}$$

where x_d is the location of the defect, t_f is the time-of-flight. It is worth highlighting that this technique cannot detect pre-existing defects that already existed prior to the installation and monitoring. Moreover, since it is based on passive sensing, it is vital for the sensors to be active prior to the generation of stress waves. As such, this technique is useful for regular health monitoring where sensors can be permanently installed. Additionally, this technique is only suitable for defect detection and localization but it cannot discern the type of defect.

In literature, numerous authors have explored the application and suitability of AET for the monitoring of fiberglass pipes. For instance, Chandarana et al. [59] conducted an experimental study on composite pipes, fabricated from a uni-directional pre-preg comprising 5 alternating layers of carbon fiber (T700) and glass fiber (E-class). They utilized four rings of PWAS[2]–PIC255, each containing 4 PZTs measuring 10 mm in diameter and 5 mm in thickness. This setup generated a 60 V voltage signal using a three-cycle tone burst in a pitch-catch configuration within a 230 to 270 kHz frequency range. Under the Longitudinal mode L(0,2), mechanical loading was performed using a three-point bending test. Their results showed that PWAS can be embedded within the structure and can serve a dual purpose — both for passive SHM and active Guided Waves NDT&E . By plotting tuning curves with the maximum amplitude, they identified spectral plots that maintained a consistent amplitude, enabling the detection of damages. Notably, they highlighted the necessity of having a baseline (pristine) data set for effective comparisons. Furthermore, an experimental setup using a hemispherical striker weighing 0.52 kg dropped from a height of 1 m, coupled with a three-point bending test, was used. The experiments encompassed 1 to 5 loading cycles, ranging from 2000 N to 9115 N, primarily focusing on delamination detection. Their result analysis indicated an amplification in signal amplitude across loading cycles, indicating the presence of delamination defects.

Wu et al. [97] presented an interesting study on three-ply pipes whose properties closely resemble those of Fiber-Reinforced Plastic (FRP). These pipes underwent non-uniform external loading and consistent internal loading. The authors employed ANSYS to validate, focusing on quantifying stresses and displacements to observe long-term deflection patterns. Their efforts contributed to developing an analytical model that particularly predicts the time-dependent mechanical behavior, emphasizing both displacement and stress, of a multilayered pipe equipped with a visco-elastic inter-layer. In addition, their investigation delved into the nuances

[2] Piezoelectric wafer active sensor.

of how the modulus ratio, load distribution, and various inter-layer parameters influenced the overall behavior and stability of the pipes.

She and Cai [80] focused on the study of composite pipes, focusing on the use of 8 PZT sensors (arranged in sets of 4) that were firmly bonded using epoxy resin and augmented with an AE analyzer DS5-8B. The pipes were subjected to a rigorous static compressional loading of 230 kN. The primary method of observation was the monitoring of longitudinal waves. The experimental setup revealed the evolution of bulges and cracks in the specimen, progressing to a state of complete fracture. The study demonstrated that when the GFRP pipe specimen was exposed to static loading, the strategically placed PZT sensors efficiently recorded the AE signals. The authors successfully computed the AE emission source location using the arrival times of these stress waves and a set of four sensors positioned horizontally and using the average longitudinal wave signals.

Another insightful study was undertaken by Yu et al. [103], who investigated pultruded fiberglass embedded in mat layers. Following the JIS K7113-1995 standards, they employed a tensile test on pipe samples with no pre-existing defects. The mechanical testing was rigorous, progressing to the point of breakage. This study made use of a square pipe configuration. The researchers quantified the fiberglass content using the calcination method, adhering to the GB/T 2577-2005 standards. Their comprehensive methodology incorporated a three-point bend test, a tensile test, a fiber content test, and dynamic mechanical analysis. Interestingly, their findings highlighted a multi-stage damage progression, specifically during the tensile loading phase.

In a numerical study by Zhao et al. [63], the SHM of a Basalt FRP pipe constructed from five plies of basalt fiber with orientations at both ±45–degrees was investigated. They incorporated a long-gauge macro strain sensor, and the ambient loading was introduced as random noise orthogonal to the pipe wall. The research utilized ANSYS [SHELL 181] for simulations, where random excitation was applied near one edge, and measurements were taken at 10 different stations across the pipe. A significant observation was the stiffness reduction observed in a 60 mm long segment across 180–360 degrees. They injected a 1-second long signal with a 1000 sampling rate. The team measured rotational displacements using angular displacement sensors at various angles. The study advanced by employing the circumferential distribution plots of modal macro strain as an input for a Convolutional Neural Network model, aiming to predict damage properties, such as location, extent, and degree represented as a scalar output.

In another numerical investigation conducted by Oke et al. [86], the dynamics of a fluid-filled laminated composite pipe were explored. This composite pipe was constructed of three-layered laminates oriented at ±54–degree plies. Utilizing wavelet-based FEM modeling, the authors sought to examine the impact of internal surface discontinuities, especially internal wall thinning, on the vibrational attributes of the structure. The study revealed that dynamic flow acceleration can lead to erosion and internal surface degradation, consequently causing wall thinning. The authors efficiently modeled the pipe-fluid system using extended Hamilton's approach. Furthermore, for the vibrational analysis, low frequencies in the range of 5 to 60 Hz were selected. One of the key takeaways from this study was the understanding that as the size of the defect grows, it diminishes the pipe wall's stiffness, subsequently lowering the pipe's natural frequencies. Another paper by the same author [87], also focused on using the Wave Based Finite Element Method (WBFEM) and ANSYS to evaluate the composite's response to pulse-type forcing. The primary goal was to derive the impulse response function and understand its implications on the internal surface discontinuities. Their results analysis highlighted the critical influence of wall thinning defects on the dynamic response. In fact, they reported that the presence of wall thinning led to amplification and a notable shift in the frequency response. From this research, the authors proposed that vibration analysis is an effective tool for monitoring erosion-induced internal defects in composite structures.

Wang et al. [104] adopted both analytical and experimental approaches to investigate the dynamics of CFRP pipes. Using externally attached FBG[3] sensors, axial strain measurements were recorded and referred to as vibrations. For the experimental setup, the pipe was positioned with cantilever support conditions, and the mathematical model was derived based on the Beam Theory. The study employed low-frequency excitation ranging from 10 to 50 Hz for the analysis. While the results showcased a commendable agreement between the theoretical and measured strain outputs regarding frequencies or wave periods, discrepancies were noted in amplitudes attributed to attenuation in the experimental signals.

The foregoing literature review highlights that AET is a potential technique that can be employed and further developed for condition assessment and health monitoring of fiberglass/composite pipes. However, several challenges are associated with its application: (1) The characteristics of waves (e.g., frequency bandwidth, amplitude, and frequency-dependent attenuation) induced by the defect are dynamic and usually unknown. As such, the low signal-to-noise ratio (SNR) issues commonly exist in this type of NDT&E ; (2) The structural composition, anisotropic nature, and non-homogeneity modify the wave propagation and induce additional complexities that are uncommon in metals. As such, the understanding of wave propagation in composite and layered structures is necessary in analyzing the collected signals. In terms of buried pipe, this technique requires similar procedures as GWUT, with the primary difference that it is based on passive sensing and thus relies on passive wave sources (e.g., mechanical vibrations induced by faulty machinery or defect progression due to intensive operational conditions).

5.5. Infrared thermography (IRT)

Infrared thermography (also known as thermal imaging) is a well-known and non-contact-based method for inspecting materials. This technique relies on the principle that every material surface with a temperature more significant than absolute zero emits electromagnetic radiation with a length scale smaller than the visible light. As such, a defect causes a unique heat distribution

[3] Fiber Bragg Grating.

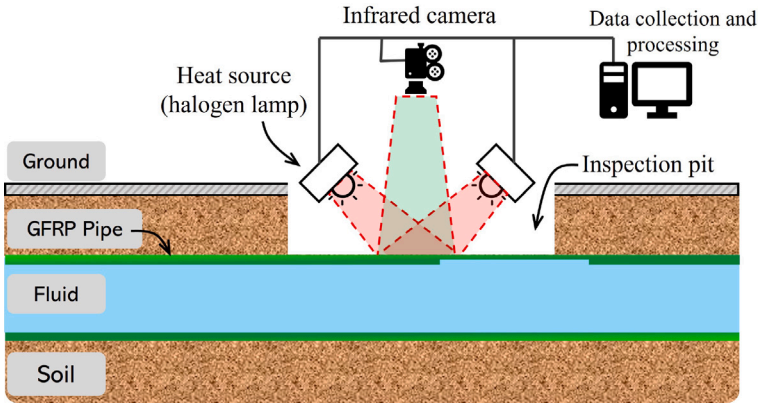

Fig. 26. Illustrative example of the infrared thermography technique. It involves a light source (e.g., halogen lamp) which produce heat in the exposed pipe section and an infrared camera which captures the heat emitted by the pipe section. The source can be a short-time pulse-like input or it can be a long-term sequence with user-defined pattern (e.g., sinusoidal).

different from the defect-free surface and can be detected and recorded using infrared cameras and correlated with baseline (defect-free) or model-based simulated results to identify the differences. This technique can be used during manufacturing and in-service stages and is suitable to detect surface and shallow-surface defects. A general rule of thumb is that a defect whose surface length is larger than its depth is detectable and undetectable otherwise. Fig. 26 illustrates the application of the IRT technique for the case of an underground pipeline system. It allows for fast inspection rates and can cover a large surface area (~few meters depending on the pit size), given that the pipeline is accessible. However, the quality of the images is susceptible to environmental noise and strongly depends on the quality of the camera. Moreover, it is suitable for near-surface defects, as the ones in the deeper layers have low rate of radiation and often remain undetected.

This technique can be deployed in both passive and active modes. In the former mode, the infrared images are collected without projecting any heat source on the surface. This mode is relatively useful during the manufacturing process, where the temperature of the FRP pipe is expected to vary. However, this mode is prone to errors for in-service pipelines as the image quality primarily relies on ambient conditions and often has a low signal-to-noise ratio (SNR). For in-service pipelines, the active mode is often utilized and is generally performed in two ways: Pulsed IRT and Lock-in IRT. In the former approach, an input heat source, such as a halogen lamp, is used to heat the target surface, and thermal images are captured with an infrared camera. This approach estimates the instant energy radiating by the surface and can detect surface and sub-surface abnormalities at shallow depths in various materials, including metals, composites, and polymers. In the latter (Lock-in IRT) approach, a periodic and modulating (user-defined pattern) heat source is projected on the specimen, and the transient thermal responses (sweep of images) of the sample are recorded with time. The phase and amplitude of the thermal images are then analyzed for the detection and quantification of defects. It is vital to note that the interpretation of thermal images requires equipment handling expertise and domain-knowledge to operate as well as to interpret the recorded images.

In literature, Gomathi and Ramkumar, in their exclusive research [88], employed infrared thermography, a lesser-explored technique, for defect detection in GFRP materials. Utilizing a focal-plane array-based Silver 420IR camera and Xenon flash lamps for their experimental setup; they concentrated on studying unidirectional E-glass winding at a 54-degree angle. The experiments were carried out under both pulsed and lock-in configurations, aiming to detect drilled holes of varying depths ranging from 0.6 mm to 4.2 mm. The study made use of thermographic signal reconstruction techniques in reflection-mode thermography. When employing lock-in thermography, a four-point correlation analysis was crucial. The camera was consistently positioned 30 cm from the specimen's surface for all tests. Notably, while the technique effectively identified shallow-depth holes, deeper ones were often missed due to insufficient thermal energy reflection.

Although this technique is widely recognized for NDT&E of structures, it has been rarely employed for inspecting fiberglass pipelines. This hesitancy likely stems from the intensive operational demands associated with this technique, such as equipment sensitivity, sensor calibration, high power consumption, and safety precautions. Additionally, it provides only a localized scan, necessitating an inspection pit that offers limited accessibility, especially for large-scale buried pipelines. Such constraints not only complicate the inspection process but also escalate both the time and cost involved. The transparency and reflective attributes of fiberglass further complicate the inspection procedures, as they can introduce challenges in discerning accurate temperature differentials, making the detection of defects or inconsistencies challenging. Consequently, while infrared thermography possesses potential, extensive research and optimization are imperative for its practical application in inspecting fiberglass pipelines.

5.6. Microwave imaging (MWI)

Microwave imaging (MWI) is an advanced NDT&E technique that is based on electromagnetic waves and dielectric properties (e.g., dielectric constant, dielectric loss, dielectric strength, electrical conductivity, and permittivity) of the test specimen. The

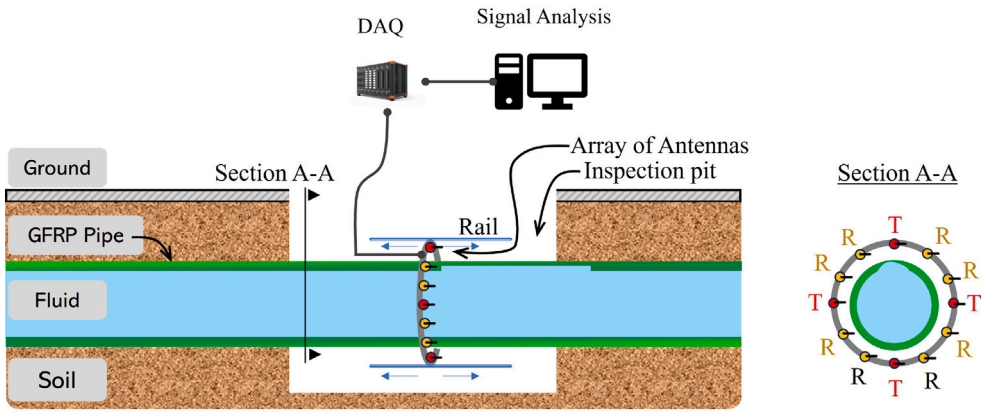

Fig. 27. Illustrative example of the microwave imaging device. It comprises of an array of antennas (used as transmitters **T** and receivers **R**), a mechanical device for roving the ring of antennas in the axial direction, and the data acquisition system (DAQ) for control and operations. The antennas can be in-contact with the exterior boundary of the pipe or lift-off (non-contact) depending on the excitation frequency, hardware capabilities, and assembly. Section A-A shows the cross-sectional view of the assembly.

working procedure of this technique is as follows. The hardware setup is comprised of a circumferential array of antennas that are placed around the pipe in the azimuthal direction with a user-defined angular spacing, allowing to scan the pipe in the azimuthal direction (see Fig. 27). The antennas are paired as transmitters (**T**) and receivers (**R**) and are uniformly distributed. This assembly of antennas are usually placed on a mechanical rover, which enables the ring of antennas to move axially and allow a longitudinal scan of the pipe, thus providing a B-scan of the specimen. As the wave propagates and interacts with anomalies, the changes in the dielectric properties introduced by the defects (e.g., fiber delamination or cracks) make the incident waves to reflect, refract, and scatter. These responses are used to investigate the health status (intact or defected) as well as to infer the defect properties (e.g., location, size, frequency). Since the transmitter and receiver used in this approach are antenna-based (operating at GHz frequencies), this technique is classified as the non-contact-based approach. The small wavelengths enable the waves to penetrate the surface, making them suitable for detecting internal and/or hidden defects.

While this technique is based on Synthetic Aperture Radar (SAR) processing for near-field imaging, its application in pipeline inspection has several challenges: (1) the technique strongly depends on the closed-form analytical solutions of the wave equations (e.g., the Green's function) which is mostly known for simple geometries with known physical pipe parameters, and (2) the antennas used for transmission and receiving the waves are modeled as point-wise. While the latter assumption is often made for convenience and computational efficiency, it brings several limitations, including the lack of antenna geometry and radiation pattern in the models, polarization mismatch, and the absence of the incorporation of near-field wavefield dynamics. Another limitation of microwave imaging, albeit passively mentioned, is the signal-to-interference ratio, which drastically reduces this technique's efficiency.

In the literature, the New York Institute of Technology (NYIT) has been at the forefront of pioneering research in microwave imaging, with several researchers contributing to its advancements. Gao et al. [26] conducted both experimental and numerical studies, focusing on PVC fluid-filled pipes filled with a mixture of 60% water and 40% glycerin. Their approach employed microwave board transmitters and receiver antenna arrays, using FEKO software for parametric studies. They employed electromagnetic waves with a center frequency of 1.7 GHz and a bandwidth of ±0.2 GHz. The authors developed the holographic near-field microwave imaging technique and applied the sLORETA approach to measured wavefields, incorporating uniform DFT and DTFT. Additionally, they utilized the Structural Similarity (SSIM) index for final output visualization. Their methodology achieved a maximum stand-off distance of 2 mm with commendable precision.

In a study conducted by Wu et al. [93], numerical and experimental research was undertaken, primarily focusing on concentric PVC pipes and drawing implications for fiberglass pipes. The method employed involved using microwave boards for the transmitter and receiver antenna arrays, with FEKO utilized for antenna design, explicitly targeting a frequency range of 6.6 – 8 GHz. The research introduced the near-field holographic microwave imaging technique tailored for concentric pipes. This method harnessed the potential of evanescent waves, facilitating sub-wavelength resolution while capitalizing on a narrow bandwidth. The authors used the Standardized Minimum Norm (SMN) approach to solve the governing equations. This study underscored the significance of obtaining baseline readings for precise defect interpretation and also delineated several pivotal factors for augmenting image quality. Nonetheless, there were acknowledged limitations, such as the prerequisite for material homogeneity and the challenges encountered in fluid-filled environments.

In a study by Amineh et al. [94], both numerical and experimental research was conducted on PVC pipes, with FEKO software playing a pivotal role in simulations and analysis. The study explored a frequency range of 8 – 12 GHz. The researchers applied microwave NDT to concentric pipes with the near-field holographic imaging technique. They utilized circular deconvolution to address the azimuthal variability inherent in cylindrical waveguides. Additionally, they employed beam-space transformation to

detect distant defects. Their study highlighted the fundamental differences between far-field and near-field holography in antenna modeling.

In the research conducted by Shah et al. [95], numerical and experimental methods were employed, focusing specifically on an outer layer made of HDPE complemented by an inner 3D-printed layer. For the numerical simulations, the FEKO software was extensively utilized. The study delved into the frequency range of 5.5 – 6.5 GHz. Their significant findings include the successful reconstruction of the thickness profile in a thick-layered nonmetallic pipe. This was achieved using the near-field holographic imaging system coupled with experimentally determined Green's functions. They elaborated on results and theoretical underpinnings for 1-D imaging along the azimuthal direction. While their approach highlighted methods from previous studies, they incorporated a rotating array strategy for their numerical simulations. Their research culminated in presenting proof-of-concept experiments specifically on composite pipes.

Besides the pioneering efforts made by the NYIT group, another study was found by Sutthaweekul and team [89], who embarked on an experimental venture, scrutinizing a pipe structure comprised of 14 layers of fiberglass complemented with a thermal barrier coating. While the experimental setup specifics remain unspecified, they employed a Wide K-band signal, oscillating between 18–26 GHz with a bandwidth spread of ± 7.5 GHz. Their research target pertained to Flat Bottom Holes with a consistent diameter of 10 mm but variable depths, ranging from 4 mm to 11.5 mm, located on the inner surface. In their innovative approach, the team combined Principal Component Analysis with Synthetic Aperture Radar (SAR) tomography to target defect characterization. They formulated a comprehensive data matrix by conducting tests to record reflections and aligning them with probe coordinates. When this matrix was projected using PCA, it allowed for the efficient identification of the Region of Interest (ROI). With the ROI outlined, time-sequential SAR tomography imaging was then applied, ensuring a thorough examination of the defects. To sharpen the fidelity of their findings, the authors embraced the long-pulsed excitation tomography method.

Murata et al. [75] also conducted an experimental study on Fiberglass Reinforced Plastic Mortar (FRPM) pipes. They utilized a line antenna for projection purposes, paired with an electro-optic (EO) sensor for reception, operating at a frequency of 2.4 GHz, specifically focusing on a single mode, TE_{00}. Their study aimed to identify the existence of foreign objects within the pipes. One of the primary findings of their research was the discovery that FRPM is inherently dielectric. This property ensures an impressively low propagation loss, approximated at about 1 dB/m, particularly when the pipe is devoid of any content. For the purpose of their tests, Microwave (MW) guided modes were instigated using line antennas. However, it is vital to understand that the inspection predominantly occurred from the pipe's interior. Thus, both the inserter and the receptor were strategically positioned at the joints. They employed a Pitch-Catch configuration, wherein any loss in transmission was interpreted as an indicator of a defect's presence.

In summary, the MWI technique has been advancing, primarily focusing on concentric pipes. Yet, several potential challenges are likely to emerge when considering its application to fiberglass pipes. Firstly, fiberglass is characterized by its consistent dielectric properties; for MWI to detect a defect, there must be a considerable change in these properties. Otherwise, anomalies would remain undetected. Secondly, the microwave's penetration depth is thickness and frequency-dependent, making it challenging to inspect the innermost layers or thicker sections of the pipeline. Another concern is the technique's sensitivity to external interference. In the context of buried pipelines, the method requires an inspection pit and an extended axial section of the pit to allow for antenna movement to obtain B-scans.

5.7. Shearography

Shearography, otherwise known as *Speckle Pattern Shearing Interferometry*, is based on optics (light wave reflections). The general working principle is as follows. An interferometer (e.g., Michelson interferometer) is placed near the test specimen. It is comprised of a light source (typically a laser or other forms of electromagnetic wave source), a beam splitter (a partially reflecting mirror), and a detector. The light source emits a single light beam on the beam splitter, which splits the incoming coherent beam into two identical sub-beams as shown in Fig. 28(a). Both sub-beams take a different path (of varying length, resulting in phase difference), one of which is targeted to the specimen surface, reflects, interferes with each other (following the principle of superposition of waves), and is projected on the detector, resulting in interfering patterns (see Fig. 28(b)). If the specimen under observation has a defect, the sub-beam projected on the defected surface will induce a phase shift, resulting in a different interference pattern on the detector than that from the specimen without any defect.

For pipeline NDT&E , it is a non-contact-based technique and can be performed in two formats: (1) a reference sample-based inspection and (2) an unloaded state-based inspection. In the former settings, a reference pipe specimen with no defect is used as an ideal case, and its image is used as a reference to compare the images obtained from defected (e.g., in-service or in-situ) pipe samples. In the latter approach, where a reference (or controlled) sample is unavailable, the same in-situ (or in-service) pipe is first inspected in its unloaded state, and the images are stored as reference. The same specimen is then mechanically (static and internal) loaded and reinspected. In either setting, the images bearing defect information typically produce fringe-like patterns on the recorded image, which are directly proportional to the deformation or defect size. Because it is based on surface strain measurements taken by projecting light waves on the test specimen, it is only efficient in detecting surface or near-surface defects with reduced accuracy for deep-surface defects [73]. For these reasons, it can be performed internally and externally. Fig. 29 illustrates the application of shearography wherein both (a) external and (b) internal interferometer configurations are demonstrated.

The interferometer configuration shown in Fig. 28 is one of the simple configurations commonly used in shearography. Many other interferometer configurations are developed according to the application and study interest, ranging from small-scale laboratory experiments to astronomical observations and from localized material testing to large-scale structural health monitoring.

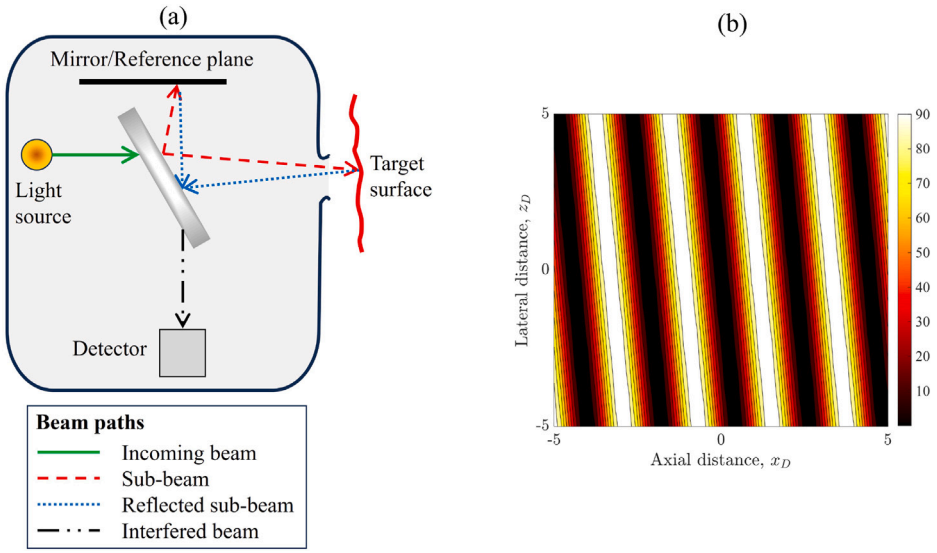

Fig. 28. (a) Configuration of Michelson's interferometer, (b) example of fringe pattern ([105] Note: the measured interference pattern is likely to be more irregular and less-dense).

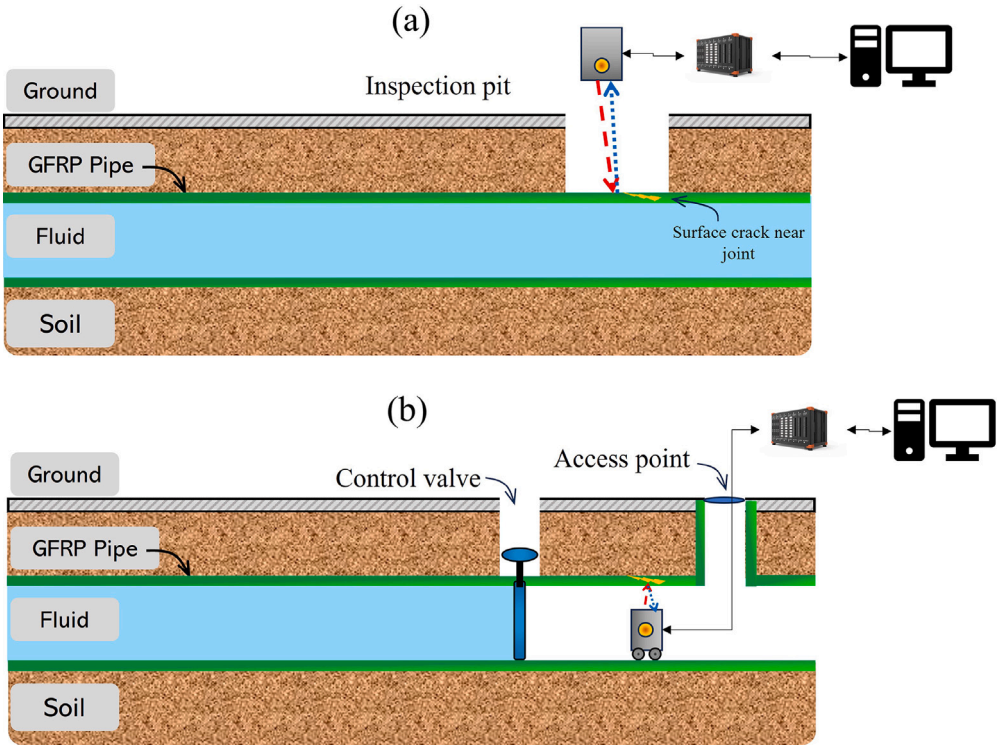

Fig. 29. (a) Shearography performed (a) externally which requires an inspection pit and (b) internally which needs a control valve to stop the flow and an access point to insert the interferometer.

In the literature, several papers relevant to the scope of this paper were found. Macedo et al. [84] developed an endoscopy shearography system using two conical mirrors that ensure radial sensitivity, vital for detecting adhesion flaws. They used a steel pipe sample featuring an internal fiberglass coating for experiments. The pipe was positioned both in open air and on a dedicated assembly to facilitate controlled inspection. Their methodology incorporated the use of COBOLT — SAMBA, equipped with a 532 nm DPSS laser boasting 1 W of power. For imaging, they employed a PointGrey FLEA 3 camera, characterized by a 2-megapixel resolution

bolstered by a CMOS sensor. Their key focus lay on adhesive flaws, more specifically, matrix-related defects. To emulate these defects, they drilled a 7 mm hole, subsequently employing a micrometric screw to establish a separation between the pipe wall and its coating. It is worth highlighting that the inspections were carried out from the inner side of the pipe. Their setup incorporated a 45-degree angled conical mirror for the primary examination and an 89-degree mirror to facilitate radial displacement. Such an arrangement permits a comprehensive 360-degree inspection of the entire pipe circumference.

Xie and Zhou [73] embarked on an experimental analysis of CFRP pipes. They also used digital shearography and employed the Michelson Interferometer for their experiments. They applied this technique to a composite tube built to withstand high pressures up to 1000 psi or 60 bars. To initiate the experiment, a baseline shearography phase map was established at 0 psi. The tube was then pressurized using an oil pump. By subtracting the two-phase images obtained at different pressures, the authors were able to identify sub-surface defects at shallow depths. These findings were further validated by comparing them with results from CT scans. A significant observation from their study was the propensity for defects to manifest at intersections where two fiber directions converged.

In summary, shearography offers a promising yet under-explored avenue compared to other techniques. Its lesser adoption can be attributed to several factors: (i) its invasive approach when used internally, making it less ideal for in-service pipelines; (ii) its limited efficacy in detecting sub-surface defects, which are critical for NDT&E of pipelines; and (iii) the inherently labor-intensive process which not only increases operational costs but also demands skilled labor due to the equipment's fragile nature.

5.8. Other NDT&E techniques

5.8.1. Electric potential technique

Altabey et al. [78] embarked on a numerical exploration into the use of electric potential technique for defect detection in basalt FRP pipes. The pipe samples were made of three layers having winding orientations set at 0, 90, and 0 degrees. As their investigative tool, the team employed Electrical Capacitance Sensors, configuring twelve of these with a spacing of 2 mm between each. By providing a 15 V electric potential input and utilizing a 2D ANSYS model, the study simulated the effects of cyclic loading to induce matrix cracking, representing fatigue-induced damage. The primary focus was on the application of the Electrical Capacitance Sensors technique, which was revealed to be only appropriate for circumferential evaluations. As an active-sensing modality, their techniques use a pulse-catch mode: one electrode is energized at any given moment, while the remaining ones act as detectors. The method enables the detection of dielectric properties, with sensors strategically affixed to the external wall of the pipe.

5.8.2. Optical microscopy

Liao et al. [12] used optical microscopy technique on GRE pipes. The sample pipe under examination comprised of E-glass fiber, mainly designed with several layers following a ±45–degree spiral winding pattern. In particular, the authors utilized the advanced scanning electron microscope, the ZEISS mini 300, in their experiments. Their examination was primarily centered on a burnout test, conforming to ASTM D2584 standards. It revealed a significant crack that spanned 10 cm in length and 3.5 cm in width, running parallel to the direction of the fiber winding. This study was particularly effective as it delved into the in-depth analysis of a GRE pipe, spanning 1.846 km, employed for 12 years to transport sewage water while buried approximately 1.5 m below ground level. This pipe encountered a sudden rupture. Their findings identified the primary culprits behind this failure as cavity defects — notably air bubbles and gaps stemming from inadequate resin filling during the manufacturing stage. Furthermore, improper curing procedures and compromised fiber bonding strength significantly contributed to the eventual pipe rupture.

5.8.3. Radiography

In an experimental research conducted by Ferreira et al. [76], radiography was employed to inspect GRE pipe samples. Their setup incorporated an X-ray tube with a 1 mm focal spot, boasting a maximum power of 1000 W. The imaging was captured through an A-Si flat panel detector with a pixel granularity of 200 μm. The authors also utilized a micro CT system with a micro-focus X-ray tube for detailed investigation. The team leveraged the ISee software for image analyses, which was particularly tailored for radiographic image assessment. For in-depth examination and rendering of the micro CT data, the CTAn and CTVox software platforms were utilized. Their study targeted defects commonly found in composite materials, specifically voids, delamination, and debonding. Radiography offered them 2D insight, whereas computed microtomography (micro CT) provided a 3D perspective, especially on hand-laid laminated joints. One intriguing discovery from their analysis was that even in a controlled sample that was presumably intact, the radiographic imagery could detect the presence of debonding and delamination, highlighting the sensitivity and capability of their chosen methodologies.

Table 3 provides an overview of the foregoing NDT&E techniques, highlighting their suitable stage of application based on practical requirements along with their benefits and limitations. In essence, NDT&E techniques for composite pipeline inspection span a spectrum of developmental stages. Emerging methodologies like the Electrical Potential Technique, Optical Microscopy, and Radiography are still in the early phases of application. In contrast, more advanced techniques such as Microwave Imaging and Infrared thermography have matured to the extent that they are ready for in-situ or real-field testing. Interestingly, Visual Inspection (VI) and Acoustic Emission Technique (AET) have already been deployed in challenging environments, favored for their straightforward implementation. GWUT, on the other hand, is still in its infancy, primarily due to the complexities in signal interpretation, the need for advanced training for operators, and challenges in accurately assessing and sizing defects in layered composite structures. Given the complex nature of composite materials and the practical challenges posed by poorly accessible pipeline locations – such as offshore or underground settings – a synergistic approach employing multiple NDT&E techniques is anticipated to be most effective. This multi-modal strategy could mitigate the limitations of methods like Shearography and Thermography, which are constrained by site accessibility, allowing versatile techniques like AET and GWUT to excel due to their adaptability to out-of-sight applications.

Table 3
Summary and overview of NDT&E techniques suitable for fiberglass pipelines.

Technique	Application type	Benefits	Limitations	Suitable stage	References
Visual Inspection	Non-contact, Non-intrusive	Simple, quick for accessible and short sections, cost-effective, offers on-site observations, no potential safety concerns	Passive, reactive, only suitable for surface/apparent defects, labor intensive, time consuming for long pipelines	Manufacturing and storage	[12,53,61,62,66,77,81–83,92]
Guided waves Ultrasonic testing	Contact-based, Non-intrusive	Offers long-range inspection, proactive, can detect sub-surface defects, suitable for diverse kinds of defects, offers quick inspection, versatile (applicable to different sizes and geometry),	Waveguide attenuation limits the range, requires skills for data analysis, often require surface preparation, relatively expensive then VI, require SNR optimization, Sensitive to defect orientation	Manufacturing, storage, in-service	[58,60,64,91,106]
Acoustic Emission Technique	Contact-based, Non-intrusive	Suitable for health monitoring, does not require active source generation, require less power for operations	Passive, reactive, only suitable for defects that generate stress waves, offers short-range monitoring, require material properties for wave speed estimation, need skilled manpower for data analysis, require surface preparation for probe installation, need SNR optimization	Manufacturing and in-service	[59,63,80,87,97,103,104]
Infrared thermography	Non-contact, Non-intrusive	Rapid, does not require complex signal processing, efficient for geometry deforming defects,	Require surface preparation, only inspect local and exposed target area, not suitable for internal and micro-scale defects, limited to near-surface external defects, sensitive to environmental conditions, costly and require power supply	Manufacturing and storage	[88]
Microwave imaging	Non-contact, Non-intrusive	Fast, offers high resolution, offers B-scans, suitable for both internal and external defects	Requires advanced signal processing and waveguide modeling, require circumferential access to the pipe, requires extended inspection pits, passive and reactive	Storage and in-service	[26,75,89,93–95]
Shearography	Contact-based, Non-intrusive and Intrusive	Efficient for surface/near-surface defects	Intrusive as it may require system shutdown, slow, not suitable for micro-scale defects,	Manufacturing and storage	[73,84]
Electric potential technique	Contact-based, non-intrusive	Rapid, detects sub-surface defects,	Sensitive to defect type, require pristine conditions, Requires advanced signal processing tools to interpret the results,	Manufacturing and storage	[78]
Optical microscopy	Non-contact, Non-intrusive	Offers high resolution, suitable for surface and near-surface defects, Provide real-time and in-situ inspection, proactive	Prone to errors for internal defects, covers low-range, slow inspection, requires skilled manpower for conducting experiments	Manufacturing and storage	[12]
Radiography	Non-contact, intrusive	Offers detailed images, suitable for micro-scale defects	Time consuming, require sample preparation, disruptive and intrusive, require special handling, Sensitive to defect orientation	Manufacturing and storage	[76]

6. Conclusion and outlook

This paper presents the multifaceted challenges and opportunities associated with the NDT&E of fiberglass-reinforced polymer (FRP) pipes utilized across multiple industrial domains. The complexities of FRP pipes arise from their distinctive manufacturing and handling protocols, potentially giving rise to a diverse range of defects. Depending on their developmental stage, these defects can

emerge during the initial manufacturing process or manifest after being placed in-service. Based on the literature review, following are the five primary findings of this study:

1. The commonly reported defects associated with composite pipelines are fiber waviness, dry spots, porosity, foreign object inclusion, inadequate resin curing, surface and impact damages, delamination, leaks, and chalking.
2. Many studies primarily focus on artificially created or engineered defects, rather than naturally occurring ones in composite pipelines.
3. There exists a lack of understanding in the interrelation and progression of defects in composite pipelines, underscoring the need for in-depth defect lifecycle analysis and failure mechanism studies.
4. Among several NDT techniques, Visual Inspection and Acoustic Emission Techniques are prevalent, with the latter advancing significantly and being adopted for challenging applications. Guided wave ultrasonic technique is also gaining traction.
5. Microwave Imaging has shown promising results in laboratory settings and for specific applications such as concentric pipelines. Its readiness for real-world implementation is anticipated, with practical field applications in the near future.

In essence, while various techniques are being actively developed and are at the forefront of research, it is accurate to say that the NDT&E methods for FRP pipelines remain in their infancy, necessitating further exploration and advancement. In light of this, the following topics are identified as crucial focal points that, if pursued, may lead to technological solutions, addressing practical challenges:

Engineered versus natural defects: The present research predominantly focuses on engineered defects (e.g., coupled coins, machined holes). However, there is a need to pay attention to naturally occurring defects in FRP pipes during all manufacturing, storage, installation, and in-service stages. Focusing on these real-world defects is crucial in assessing the performance of NDT&E techniques. In addition, most of the existing research is based on laboratory conditions, which might not truly represent the complexities and variables of in-field scenarios. Therefore, extensive field studies, together with advanced NDT&E techniques tailored to detect and analyze naturally occurring defects, are of paramount importance. By bridging this gap, the pipeline industry can have more confidence in utilizing FRP pipelines.

Inspection length scales: Most studies have examined pipe samples limited to approximately 1 m in length. While this serves as a preliminary foundation, it is essential to remember that piping systems typically extend over vast distances (on the order of kilometers). In such a context, there is a pressing need to develop NDT&E techniques capable of detecting defects in large-scale pipelines. Low-frequency hydraulic transient waves [96,107], previously developed for metallic and polyethylene pipe systems, appear promising because they propagate over long distances ($\sim 10^2$ m) when excited within the fluid. It is anticipated that a synergistic approach, integrating low-frequency transient waves with high-frequency ultrasonic waves and subsequently complemented by techniques like microwave imaging, Shearography, or infrared thermography, could provide a more pragmatic solution.

Fluid-borne waves: In most wave-based techniques, the primary focus has been structure-borne waves. While this approach has received significant attention, it is essential to note that these waves often experience significant damping, especially considering that most piping systems are buried. Consequently, the injected waves dissipate into the surrounding environment (like soil) or the internal fluid, which can lead to a limited propagation range. On the other hand, fluid-borne waves [108–110] present a compelling solution to this challenge. Given their ability to mitigate the effects of excessive damping, they possess the potential to emerge as a viable technology for inspecting and imaging pipelines over extended distances. It might also be advantageous to explore how fluid-borne waves can be efficiently harnessed in conjunction with other inspection technologies to improve the accuracy and reliability of pipeline assessments.

In-service FRP assessment: A large portion of the existing research is laboratory-centric. While controlled laboratory environments offer insights into understanding defect mechanics and how different defects induce different signatures for specific NDT techniques, real-world conditions present a myriad of variables that cannot always be emulated in the lab. For instance, factors such as harsh environmental conditions, external loads, ground movements, and prolonged wear and tear, which can profoundly affect the behavior and health of FRP pipes, are challenging to simulate in laboratory settings. Therefore, the forthcoming task should be made on inspecting in-service pipes, prioritizing continuous monitoring, and condition assessment.

Damage severity metric: While a wide range of NDT&E techniques is found in the literature; it has been noted that a standardized metric for damage severity – crucial for determining the action threshold for repairs or replacement – is not prominently featured within the surveyed literature. This highlights a potential gap in the current research landscape. Recognizing the significance of such metrics in pipeline integrity management, it is suggested that future studies should aim to develop and define comprehensive damage severity metrics tailored for composite pipelines to better guide the selection and application of NDT techniques.

Proactive and not reactive: While most of the existing research focuses on detecting pre-existing defects, which is a reactive approach, there is a need to shift the research paradigm to a more proactive approach. This proactive approach would identify early-stage anomalies and potential issues before they mature into significant defects, potentially leading to system failures or shutdowns. Addressing these challenges pro-actively can significantly enhance the reliability and longevity of FRP pipelines, ensuring safer, reliable, and more efficient operations.

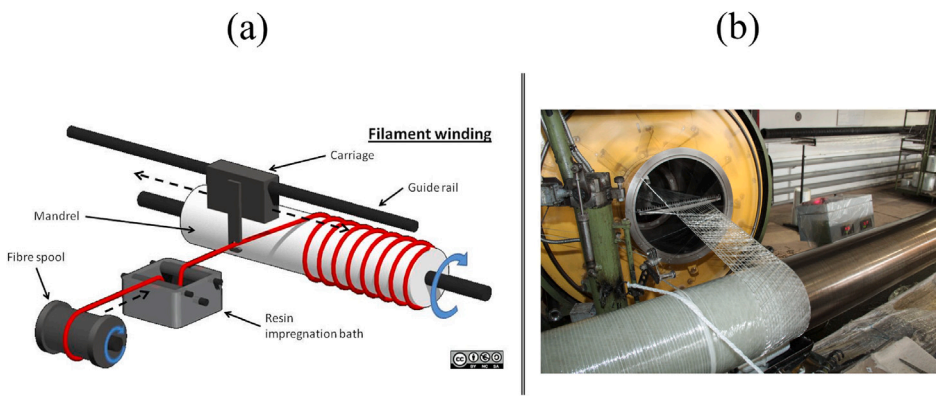

Fig. A.30. An illustration of the filament winding process (a) overall working stages of the process and (b) a real-time winding process. The left figure shows the fibers being pulled from the spool, impregnated with resin, and wounded on the mandrel guided by a carriage. These figures are obtained from Google Images under creative common licenses: (a) CC BY-NC-SA 2.0 by [112], and (b) CC-BY-SA-3.0 by [113].

Besides the directions highlighted, there is noteworthy potential in integrating SHM and NDT techniques for a proactive approach in composite pipeline monitoring. SHM-based techniques such as fiber optics, PZT sensors, and acoustic emissions could complement active probing methods. This dual approach, not extensively covered in this paper, opens promising avenues for future research in pipeline integrity management.

CRediT authorship contribution statement

Muhammad Waqar: Conceptualization, Data curation, Formal analysis, Investigation, Methodology, Software, Validation, Visualization, Writing – original draft, Writing – review & editing. **Azhar M. Memon:** Writing – review & editing, Supervision, Resources, Investigation, Conceptualization. **Muhammad Sabih:** Writing – review & editing, Visualization, Data curation, Conceptualization. **Luai M. Alhems:** Writing – review & editing, Supervision, Project administration.

Declaration of competing interest

The authors declare that they have no known competing financial interests or personal relationships that could have influenced the work reported in this paper.

Data availability

Data will be made available on request.

Declaration of Generative AI and AI-assisted technologies in the writing process

During the preparation of this work the authors used ChatGPT (v4.0) in order to rephrase some sentences for enhanced readability. After using this tool, the author reviewed and edited the content as needed and take full responsibility for the content of the publication.

Appendix A. FRP pipe fabrication methods

There are several different methods to fabricate FRP pipes. The common methods include (i) filament winding, (ii) centrifugal casting, (iii) pultrusion, (iv) hand lay-up, and (v) spray-up. A brief description of each method is provided below.

A.1. Filament winding

Filament winding process is widely used in the fabrication of FRP pipes [111]. In this method, fibers, such as glass or carbon, are wound onto a rotating mandrel in a precise and continuous pattern. As the fibers are wound onto the mandrel, they are impregnated with resin, typically epoxy. The pipe is then cured to solidify the composite. Fig. A.30 demonstrate the simplest configuration of filament winding process along with a real-time image of the winding mandrel.

Fig. A.31. An illustration of the centrifugal casting process is shown, providing an inner view of a steel mold.

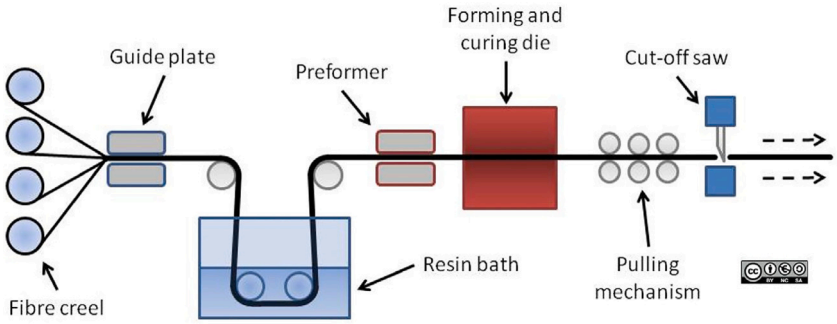

Fig. A.32. An illustration of the Pultrusion process. After being pulled from the creel, the fibers are penetrated into the resin and pased through the "preformer" to align the fibers in the desired form. The forming and curing die is used to remove the excessive resin and for curing the sample. The cured samples are pulled forward by the rollers and a cut-off saw is used to cut the section as per the desired length. Image obtained from [115] under the Creative Common License CC BY-NC-SA 2.0.

A.2. Centrifugal casting

In this process, a pipe mold is rotated at high speeds while the liquid resin and fiber reinforcement are poured into the mold (as shown in Fig. A.31). The centrifugal force generated by the rotation causes the resin to spread evenly and uniformly along the inner surface of the mold, ensuring that the resulting pipe has a consistent thickness and uniform fiber distribution. More details on the centrifugal casting technique can be found in [114].

A.3. Pultrusion

In this technique fiber reinforcements rovings are continuously pulled and impregnated with resin bath cured simultaneously as depicted in Fig. A.32. As such, this technique is useful for producing products that are long and maintain a consistent shape.

A.4. Hand lay-up

This is a manual process where layers of fiber reinforcements, such as woven fabrics or chopped strands, are placed by hand onto a mold or mandrel. Resin is then applied to impregnate the fibers, and the composite is allowed to cure. This process is commonly used to manufacture pipe fittings. Fig. A.33 (left) demonstrate the hand lay-up procedure which involve (i) mold cleaning, (ii) application of resin coating followed by successive layers of resin and fiber, (iii) curing by heating and (vi) removing from mold.

A.5. Spray-up process

In spray-up method, chopped fibers (strands) and liquid resin are simultaneously sprayed onto a mold or mandrel using specialized equipment. The sprayed mixture is evenly distributed and compacted to form the pipe/fitting shape. Fig. A.33 (right) demonstrate the simplified layout of spray-up procedure.

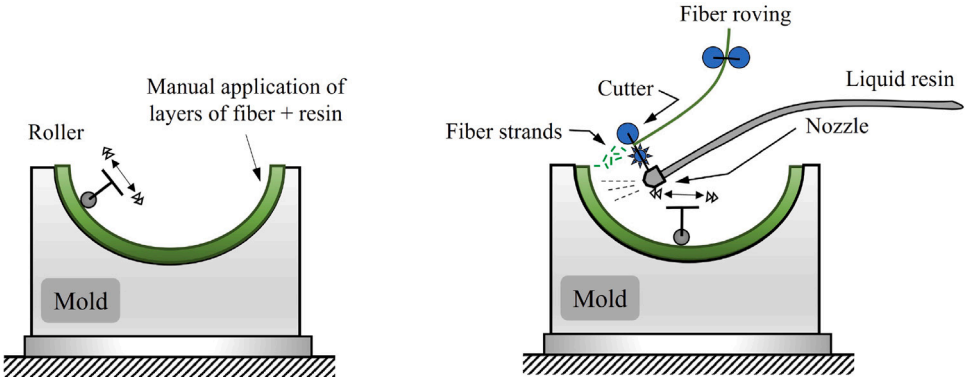

Fig. A.33. An illustration of the hand lay-up fabrication (left) and spray lay-up fabrication (right) fabrication of FRP material.

Table B.4
Examples of Standards for the design and manufacturing of GRP pipelines from different organizations and for different applications.

Standard (Country of origin)	Title	Scope of application
ASTM D2992 (USA)	Practice for obtaining hydrostatic or pressure design basis for "Fiberglass" (Glass-Fiber-Reinforced Thermosetting-Resin) Pipe and Fittings	Defines procedures for hydrostatic design basis of fiberglass piping under specific pressure conditions
ASTM D3517 (USA)	Specification for "Fiberglass" (Glass-Fiber-Reinforced Thermosetting-Resin) Pressure Pipe	For fiberglass piping intended for buried water conveyance systems with internal pressure up to 450 psi
ASTM D3262 (USA)	Specification for "Fiberglass" (Glass-Fiber-Reinforced Thermosetting-Resin) Sewer Pipe	For machine-made fiberglass pipe for gravity-flow systems, including sanitary sewage and storm water conveyance, suited for buried installations and other applications such as jacking and tunnel lining
ISO 14692	Petroleum and natural gas industries — Glass-reinforced plastics (GRP) piping — Parts 1–4	Outlines the applications, pressure rating, product classification, and design envelope for GRP piping systems, primarily for offshore and onshore industrial use including produced-water and firewater systems
AWWA M45 (USA)	Fiberglass Pipe Design	Provides guidance on the design, specification, procurement, installation, and understanding of fiberglass pipe and fittings, with emphasis on utility and municipal applications
API 15HR (USA)	High-pressure Fiberglass Line Pipe	Specifies requirements for high-pressure fiberglass line pipe with pressure ratings from 3.45 to 34.5 MPa, for oil and gas production, covering dimensions, performance, design, and testing
API 15LR (USA)	Specification for low pressure Fiberglass line pipe and fittings	Details standards for filament wound and centrifugally cast fiberglass line pipe and fittings, suitable for diameters up to 24 inches and operating pressures up to 1000 PSI, focusing on cyclic and static pressures
ASME B31 (USA)	Process piping	Provides guidelines for the design, fabrication, assembly, and inspection of piping systems typically used in petroleum refineries, chemical plants, and related industrial facilities, covering a wide range of fluids and processing stages

These methods may vary in terms of complexity, production speed, and the specific properties of the resulting FRP pipes. The selection of the casting method depends on factors such as the desired pipe specifications, production volume, and cost considerations.

Appendix B. Standards for GRP pipelines

Table B.4 provides some of the design and manufacturing standards for GRP pipelines for different applications. Table B.5 provides some examples of standard for the destructive testing of composites.

Table B.5
Examples of Standards for the destructive testing of fiberglass.

Standard (Country)	Title
ASTM D638 (USA)	Standard Test Method for Tensile Properties of Plastics
ASTM D1599 (USA)	Standard Test Method for Resistance to Short-Time Hydraulic Pressure of Plastic Pipe, Tubing, and Fittings
ASTM D2105 (USA)	Standard Test Method for Longitudinal Tensile Properties of "Fiberglass" (Glass-Fiber-Reinforced Thermosetting-Resin) Pipe and Tube
ASTM 2196 (USA)	Standard Test Methods for Rheological Properties of Non-Newtonian Materials by Rotational Viscometer
ASTM D2412 (USA)	Standard Test Method for Determination of External Loading Characteristics of Plastic Pipe by Parallel-Plate Loading
ASTM 2584 (USA)	Standard Test Method for Ignition Loss of Cured Reinforced Resins
ASTM D2924 (USA)	Standard Test Method for External Pressure Resistance of "Fiberglass" (Glass-Fiber-Reinforced Thermosetting-Resin) Pipe
ASTM D3262 (USA)	Standard Specification for "Fiberglass" (Glass-Fiber-Reinforced Thermosetting-Resin) Sewer Pipe
ASTM D3517 (USA)	Standard Specification for "Fiberglass" (Glass-Fiber-Reinforced Thermosetting-Resin) Pressure Pipe
ASTM D3754 (USA)	Standard Specification for "Fiberglass" (Glass-Fiber-Reinforced Thermosetting-Resin) Sewer and Industrial Pressure Pipe
ASTM D4161 (USA)	Standard Specification for "Fiberglass" (Glass-Fiber-Reinforced Thermosetting-Resin) Pipe Joints Using Flexible Elastomeric Seals.
CEN EN 2561 (Europe)	Aerospace series - Carbon fiber reinforced plastics - Unidirectional laminates - Tensile test parallel to the fiber direction
DIN 65466 (Germany)	Aerospace; fiber reinforced plastics; testing of unidirectional laminates; determination of shear strength and shear modulus in tension
DIN 65629 (Germany)	Aerospace; fabric sheet and tape prepreg from carbon fibers and non-reactive thermoplastics; technical specification
GB/T 41494 (China)	Aluminum alloy plastic lined composite pipes and fittings
GB/T 42920 (China)	Plastics - Evaluation of fire resistance properties and fire performance of fiber reinforced plastic composites
GB/T 43005 (China)	Continuous fiberglass tape wrapped reinforced polyethylene composite pipe for water supply

References

[1] L.S. McNeill, M. Edwards, Iron pipe corrosion in distribution systems, J.-Am. Water Works Assoc. 93 (7) (2001) 88–100.
[2] T.E. Perez, Corrosion in the oil and gas industry: an increasing challenge for materials, Jom 65 (8) (2013) 1033–1042.
[3] S. Radhakrishnan, B. Dyer, M. Kashtalyan, A. Akisanya, I. Guz, C. Wilkinson, Analysis of bolted flanged panel joint for GRP sectional tanks, Appl. Compos. Mater. 21 (2014) 247–261.
[4] A.F. Colombo, B.W. Karney, Energy and costs of leaky pipes: Toward comprehensive picture, J. Water Resour. Plan. Manag. 128 (6) (2002) 441–450.
[5] A.O. Bukhari, M. Bashar, A.S. Aladawy, S.L. Goh, P. Sarmah, Review of non-metallic pipelines in oil & gas applications-challenges & way forward, in: International Petroleum Technology Conference, IPTC, 2022, D031S083R001.
[6] R. Stokke, Use of glass fiber-reinforced plastics (Grp) in seawater pipe system offshore, in: Offshore Technology Conference, OnePetro, 1988, pp. 527–536.
[7] A.A. Hassen, U.K. Vaidya, F. Britt, Structural integrity of fiber reinforced plastic piping, Mater. Eval. 73 (7) (2015).
[8] D.K. Rajak, P.H. Wagh, E. Linul, Manufacturing technologies of carbon/glass fiber-reinforced polymer composites and their properties: A review, Polymers 13 (21) (2021) 3721.
[9] S.D. Curran, White Paper: Fiberglass Tank & Piping Fundamentals, Tech. Rep., Fiberglass Tank and Pipe Institute, 8252 S. Harvard Avenue, Suite 102, Tulsa, OK 74137, 2013, p. 2.
[10] P. Cousin, M. Hassan, P. Vijay, M. Robert, B. Benmokrane, Chemical resistance of carbon, basalt, and glass fibers used in FRP reinforcing bars, J. Compos. Mater. 53 (26–27) (2019) 3651–3670.
[11] S. Bobba, Z. Leman, E. Zainuddin, S. Sapuan, Failures analysis of E-glass fibre reinforced pipes in oil and gas industry: a review, in: IOP Conference Series: Materials Science and Engineering, IOP Publishing, 2017, 012004.
[12] D. Liao, B. Huang, J. Liu, X. Qian, F. Zhao, J. Wang, Failure analysis of glass fiber reinforced composite pipe for high pressure sewage transport, Eng. Fail. Anal. 144 (2023) 106938.
[13] K. Senthil, A. Arockiarajan, R. Palaninathan, B. Santhosh, K. Usha, Defects in composite structures: Its effects and prediction methods–A comprehensive review, Compos. Struct. 106 (2013) 139–149.
[14] M.A. Machado, K.-N. Antin, L.S. Rosado, P. Vilaça, T.G. Santos, Contactless high-speed eddy current inspection of unidirectional carbon fiber reinforced polymer, Composites B 168 (2019) 226–235.
[15] B. Wang, S. Zhong, T.-L. Lee, K.S. Fancey, J. Mi, Non-destructive testing and evaluation of composite materials/structures: A state-of-the-art review, Adv. Mech. Eng. 12 (4) (2020) 1687814020913761.
[16] Y. Fu, X. Yao, A review on manufacturing defects and their detection of fiber reinforced resin matrix composites, Composites C 8 (2022) 100276.
[17] J. Chen, Z. Yu, H. Jin, Nondestructive testing and evaluation techniques of defects in fiber-reinforced polymer composites: A review, Front. Mater. 9 (2022) 655.
[18] O. Okolie, J. Latto, N. Faisal, H. Jamieson, A. Mukherji, J. Njuguna, Manufacturing defects in thermoplastic composite pipes and their effect on the in-situ performance of thermoplastic composite pipes in oil and gas applications, Appl. Compos. Mater. 30 (1) (2023) 231–306.
[19] F.L. Matthews, R.D. Rawlings, Composite Materials: Engineering and Science, Woodhead Publishing, 1999.
[20] R. Unnthòrsson, M. Jonsson, T. Runarsson, NDT methods for evaluating carbon fiber composites, in: Proceedings of the Composites Testing and Model Identification, 2004, pp. 21–23, Comptest.net.
[21] N.P. Cheremisinoff, P.N. Cheremisinoff, Fiberglass Reinforced Plastics: Manufacturing Techniques and Applications, William Andrew, 1995.
[22] P.E. Irving, C. Soutis, Polymer Composites in the Aerospace Industry, Elsevier, 2014.
[23] J.M. Stickel, M. Nagarajan, Glass fiber-reinforced composites: from formulation to application, Int. J. Appl. Glass Sci. 3 (2) (2012) 122–136.
[24] A. Assi, GRP pipeline failure, 2020, pp. 58–71.
[25] C.J. Neto, Future challenges in non-metallics from an O&G industry perspective, Reinf. Plast. 65 (6) (2021) 50–53.
[26] Y. Gao, M. Ravan, R. K. Amineh, Fast, robust, and low-cost microwave imaging of multiple non-metallic pipes, Electronics 10 (15) (2021) 1762.
[27] C. Garnier, M.-L. Pastor, F. Eyma, B. Lorrain, The detection of aeronautical defects in situ on composite structures using Non Destructive Testing, Compos. Struct. 93 (5) (2011) 1328–1336.
[28] I. Scott, C. Scala, A review of non-destructive testing of composite materials, NDT Int. 15 (2) (1982) 75–86.
[29] Z. Su, L. Ye, Y. Lu, Guided Lamb waves for identification of damage in composite structures: A review, J. Sound Vib. 295 (3–5) (2006) 753–780.
[30] S. Gholizadeh, A review of non-destructive testing methods of composite materials, Procedia Struct. Integr. 1 (2016) 50–57.
[31] J. Williams, Oil industry experiences with fiberglass components, in: Offshore Technology Conference, Offshore Technology Conference, 1987.

[32] T. Carlson, D. Ordéus, M. Wysocki, L.E. Asp, CFRP structural capacitor materials for automotive applications, Plast. Rubber Compos. 40 (6–7) (2011) 311–316.
[33] M. Motavalli, C. Czaderski, A. Schumacher, D. Gsell, Fibre reinforced polymer composite materials for building and construction, in: Textiles, Polymers and Composites for Buildings, Elsevier, 2010, pp. 69–128.
[34] N.M. Telang, C. Dumlao, A.B. Mehrabi, A.T. Ciolko, J. Gutierrez, Field Inspection of In-Service FRP Bridge Decks, Transportation Research Board, 2006.
[35] G. Marsh, Composite pipes capture water and sewage markets, Reinf. Plast. 53 (6) (2009) 18–21.
[36] J.H. Mallinson, Corrosion-Resistant Plastic Composites in Chemical Plant Design, CRC Press, 2020.
[37] K.P. Baidya, S. Ramakrishna, M. Rahman, A. Ritchie, Z.-M. Huang, An investigation on the polymer composite medical device - External fixator, J. Reinf. Plast. Compos. 22 (6) (2003) 563–590.
[38] L.S. Lee, R. Jain, The role of FRP composites in a sustainable world, Clean Technol. Environ. Policy 11 (3) (2009) 247–249.
[39] J. LeBlanc, G. Palsson, Large diameter fiberglass pipes in pressure applications: ASCE pipeline 2013 - fort worth, texas, in: Pipelines 2013, American Society of Civil Engineers, 2013.
[40] B. Standard, B. Iso, Petroleum and Natural Gas Industries Glass Reinforced Plastics (GRP) Piping, BS EN ISO, 2002, pp. 14692–2.
[41] Verified Market Search, Global FRP/GRP/GRE Pipe Market Size By Product (Polyester, Epoxy), By Application (Oil and Gas, Sewage Pipe), By Geographic Scope And Forecast, Report on FRP Pipe Market Size and Forecast, 2022, Published on: 2022-07. Accessed on: 2023-05-30. Available at https://www.verifiedmarketresearch.com/product/frp-grp-gre-pipe-market/.
[42] G. Marsh, Composite pipes capture water and sewage markets, Reinf. Plast. 53 (6) (2009) 18–21.
[43] J. LeBlanc, M. Sternisha, Fiberglass pipe is helping solve the world's drinking water shortage, in: Pipelines 2016, 2016, pp. 1589–1599.
[44] J.G. Williams, Oil industry experiences with fiberglass components, in: Offshore Technology Conference, OnePetro, 1987.
[45] W. Badeghaish, M. Noui-Mehidi, O. Salazar, The future of nonmetallic composite materials in upstream applications, in: SPE Gas & Oil Technology Showcase and Conference, OnePetro, 2019.
[46] K. van Haaren, Opportunities for composites in water desalination, Reinf. Plast. 54 (2) (2010) 38–40.
[47] A. Chakraverty, S. Dash, H. Maharana, S. Beura, U. Mohanty, A novel investigation on durability of GRE composite pipe for prolonged sea water transportation, Compos. Commun. 17 (2020) 42–50.
[48] F.T. Wallenberger, J.C. Watson, H. Li, Glass fibers, Composites (2001) 27–34.
[49] F.T. Wallenberger, P.A. Bingham, Fiberglass and glass technology, in: Energy-Friendly Compositions and Applications, Springer, 2010.
[50] R.L. Hausrath, A.V. Longobardo, High-strength glass fibers and markets, in: Fiberglass and Glass Technology: Energy-Friendly Compositions and Applications, Springer, 2010, pp. 197–225.
[51] T. Sathishkumar, S. Satheeshkumar, J. Naveen, Glass fiber-reinforced polymer composites–a review, J. Reinf. Plast. Compos. 33 (13) (2014) 1258–1275.
[52] A. ten Busschen, M. Bennink, Characterisation of glass fibre reinforced expoxy (GRE) composites in hot/wet conditions, 2020.
[53] G. Qi, D. Qi, Q. Bai, H. Li, B. Wei, N. Ding, D. Zhang, X. Shao, Failure analysis on pressure leakage of FRP, Fibers Polym. 20 (2019) 595–601.
[54] M.P. Groover, Fundamentals of Modern Manufacturing: Materials, Processes, and Systems, John Wiley & Sons, 2020.
[55] D.A. Willoughby, Plastic Piping Handbook, McGraw-Hill Education, 2002.
[56] J. Trinoskey, F.A. Brahmi, C. Gall, Zotero: A product review, J. Electron. Resour. Med. Libr. 6 (3) (2009) 224–229.
[57] N.J. Van Eck, L. Waltman, Vosviewer manual, in: Manual for VOSviewer version, Vol. 1, 2011.
[58] M. Gresil, A. Poohsai, N. Chandarana, Guided wave propagation and damage detection in composite pipes using piezoelectric sensors, Procedia Eng. 188 (2017) 148–155.
[59] N. Chandarana, M. Gresil, C. Soutis, Damage detection and monitoring in composite pipes using piezoelectric sensors, in: 9th European Workshop on Structural Health Monitoring, EWSHM 2018, 2018.
[60] S. Carrino, A. Maffezzoli, G. Scarselli, Active SHM for composite pipes using piezoelectric sensors, Mater. Today 34 (2021) 1–9.
[61] J. Shi, Z. Ge, Z. Ni, J. Zheng, Burst pressure of glass fiber tape reinforced polyethylene pipes with interlayer delamination defect, J. Press. Vessel Technol. 143 (6) (2021).
[62] J.S. León, O.A. González-Estrada, A. Pertuz, Damage in fibreglass composite laminates used for pipes, in: Key Engineering Materials, Vol. 774, Trans Tech Publ, 2018, pp. 155–160.
[63] Y. Zhao, M. Noori, W.A. Altabey, R. Ghiasi, Z. Wu, Deep learning-based damage, load and support identification for a composite pipeline by extracting modal macro strains from dynamic excitations, Appl. Sci. 8 (12) (2018) 2564.
[64] S. Joas, W. Essig, F. Fröhlich, M. Kreutzbruck, CFRP pipe inspection by means of air-coupled ultrasound, in: AIP Conference Proceedings, Vol. 2055, AIP Publishing LLC, 2019, 120003.
[65] I. Papa, V. Lopresto, A. Langella, Ultrasonic inspection of composites materials: Application to detect impact damage, Int. J. Lightweight Mater. Manuf. 4 (1) (2021) 37–42.
[66] A.A. Abd-Elhady, A. Meroufel, H.E.-D.M. Sallam, M. Atta, Experimental and numerical determination of critical osmotic blister size affecting the strength of aged FRP seawater pipe, Polym. Polym. Compos. 29 (5) (2021) 456–469.
[67] A.D. ASTM, 2563: Standard practice for classifying visual defects in glass-reinforced plastic laminate parts, 2008.
[68] ASTM, Standard specification for "Fiberglass" (Glass-fiber-reinforced thermosetting-resin) sewer and industrial pressure pipe, 2019.
[69] S.W. Tsai, E.M. Wu, A general theory of strength for anisotropic materials, J. Compos. Mater. 5 (1) (1971) 58–80.
[70] Z. Hashin, Fatigue failure criteria for unidirectional fiber composites, J. Appl. Mech. 47 (4) (1980) 329–334.
[71] U. Icardi, S. Locatto, A. Longo, Assessment of recent theories for predicting failure of composite laminates, Appl. Mech. Rev. 60 (2) (2007) 76–86, http://dx.doi.org/10.1115/1.2515639, arXiv:https://asmedigitalcollection.asme.org/appliedmechanicsreviews/article-pdf/60/2/76/5441751/76_1.pdf.
[72] K. Potter, B. Khan, M. Wisnom, T. Bell, J. Stevens, Variability, fibre waviness and misalignment in the determination of the properties of composite materials and structures, Composites A 39 (9) (2008) 1343–1354.
[73] X. Xie, Z. Zhou, Shearographic Nondestructive Testing for High-Pressure Composite Tubes, Tech. Rep., SAE Technical Paper, 2018.
[74] C.H. Park, L. Woo, Modeling void formation and unsaturated flow in liquid composite molding processes: a survey and review, J. Reinf. Plast. Compos. 30 (11) (2011) 957–977.
[75] H. Murata, T. Okuda, M. Hazama, Nondestructive infrastructure measurement using microwave guided-mode propagation and reflection along fiber-reinforced plastic mortal pipe wall in underground pipeline, in: 2018 IEEE Conference on Antenna Measurements & Applications (CAMA), IEEE, 2018, pp. 1–3.
[76] C. Ferreira, R. Lopes, T. dos Santos, D. Oliveira, F. Martins, G. Pereira, Non-destructive inspection of laminated pipe joints in polymeric composite material reinforced by fiberglass, Nucl. Instrum. Methods Phys. Res. A 954 (2020) 161154.
[77] Z. Ren, L. Liu, Y. Liu, J. Leng, Damage and failure in carbon fiber-reinforced epoxy filament-wound shape memory polymer composite tubes under compression loading, Polym. Test. 85 (2020) 106387.
[78] W.A. Altabey, M. Noori, Detection of fatigue crack in basalt FRP laminate composite pipe using electrical potential change method, in: Journal of Physics: Conference Series, Vol. 842, IOP Publishing, 2017, 012079.
[79] H. Ding, A. Zhang, H. Li, D. Qi, G. Qi, N. Ding, Analysis of bulge failure of steel wire-reinforced thermoplastic composite pipe, Eng. Fail. Anal. 148 (2023) 107232.
[80] Y. She, G. Cai, Damage localization test of civil GFRP material based on acoustic emission, Saudi J. Eng. Technol. 6 (2) (2021) 32–36.

[81] A. Samanci, A. Avci, N. Tarakcioglu, Ö.S. Şahin, Fatigue crack growth of filament wound GRP pipes with a surface crack under cyclic internal pressure, J. Mater. Sci. 43 (2008) 5569–5573.
[82] E. Mahdi Saad, S. Gowid, J.J. Cabibihan, Rupture of an industrial GFRP composite mitered elbow pipe, Polymers 13 (9) (2021) 1478.
[83] M.A.A. Bakar, Z. Mustaffa, N.N. Idris, M.E.A.B. Seghier, Experimental program on the burst capacity of reinforced thermoplastic pipe (RTP) under impact of quasi-static lateral load, Eng. Fail. Anal. 128 (2021) 105626.
[84] F.J. Macedo, M.E. Benedet, A.V. Fantin, D.P. Willemann, F.A.A. da Silva, A. Albertazzi, Inspection of defects of composite materials in inner cylindrical surfaces using endoscopic shearography, Opt. Lasers Eng. 104 (2018) 100–108.
[85] N. Chandarana, C. Soutis, M. Gresil, Damage detection in composite pipes during mechanical three point bending, in: Struct. Health Monitor., International Workshop on Structural Health Monitoring (IWSHM), 2017, pp. 1429–1436.
[86] W.A. Oke, Y.A. Khulief, Effect of internal surface damage on vibration behavior of a composite pipe conveying fluid, Compos. Struct. 194 (2018) 104–118.
[87] W.A. Oke, Y.A. Khulief, Dynamic response analysis of composite pipes conveying fluid in the presence of internal wall thinning, J. Eng. Mech. 146 (10) (2020) 04020118.
[88] R. Gomathi, K. Ramkumar, Defect size characterization in unidirectional curved GFRP composite by TSR processed pulse and lock in thermography: A comparison study, J. Manuf. Eng. 18 (1) (2023) 030–036.
[89] R. Sutthaweekul, G. Tian, Z. Wang, F. Ciampa, Microwave open-ended waveguide for detection and characterisation of FBHs in coated GFRP pipes, Compos. Struct. 225 (2019) 111080.
[90] J. Bingham, M. Hinders, Lamb wave detection of delaminations in large diameter pipe coatings, Open Acoust. J. 2 (1) (2009).
[91] P.D. de Almeida, G.R. Pereira, Phased array inspection of glass fiber reinforced polymers pipeline joints, J. Mater. Res. Technol. 8 (5) (2019) 4736–4740.
[92] I.Y. Sulu, S. Temiz, Failure and stress analysis of internal pressurized composite pipes joined with sleeves, J. Adhes. Sci. Technol. 32 (8) (2018) 816–832.
[93] H. Wu, M. Ravan, R. Sharma, J. Patel, R.K. Amineh, Microwave holographic imaging of nonmetallic concentric pipes, IEEE Trans. Instrum. Meas. 69 (10) (2020) 7594–7605.
[94] R.K. Amineh, M. Ravan, R. Sharma, Nondestructive testing of nonmetallic pipes using wideband microwave measurements, IEEE Trans. Microw. Theory Tech. 68 (5) (2020) 1763–1772.
[95] M.B. Shah, Y. Gao, M. Ravan, R.K. Amineh, Quantitative defect size evaluation in fluid-carrying nonmetallic pipes, IEEE Trans. Microw. Theory Tech. 70 (8) (2022) 4071–4081.
[96] M. Waqar, M. Louati, M.S. Ghidaoui, Time-reversal technique for pipeline defect detection, Water Res. (2023) 120375.
[97] P. Wu, M. Wang, H. Fang, Exact solution for infinite multilayer pipe bonded by viscoelastic adhesive under non-uniform load, Compos. Struct. 259 (2021) 113240.
[98] S. Kadam, Failure criteria for evaluating Strength of Adhesive joints, 2014.
[99] J.L. Rose, Ultrasonic Waves in Solid Media, Acoustical Society of America, 2000.
[100] J. Achenbach, Wave Propagation in Elastic Solids, Elsevier, 2012.
[101] T. Kundu, Ultrasonic Nondestructive Evaluation: Engineering and Biological Material Characterization, CRC Press, 2003.
[102] E. ASTM, 1118, Standard practice for acoustic emission examination of reinforced thermosetting resin pipe (RTRP), 2005.
[103] L. Yu, G. Liu, W. Wang, H. Hamada, Y. Yang, Mechanical failure analysis of pultrusion glass fiber pipe based on acoustic emission technology, Polym. Compos. 44 (4) (2023) 2196–2204.
[104] H.-P. Wang, S.-Y. Feng, X.-S. Gong, Y.-X. Guo, P. Xiang, Y. Fang, Q.-M. Li, Dynamic performance detection of CFRP composite pipes based on quasi-distributed optical fiber sensing techniques, Front. Mater. 8 (2021) 683374.
[105] S.S. Rao, Michelson interferometer fringe pattern, in: Central File Exchange, 2023.
[106] Z. Yang, Z. Wu, Guided waves dispersion analysis in composite pipe using the safe method, in: European Workshop on Structural Health Monitoring: Special Collection of 2020 Papers-Volume 1, Springer, 2021, pp. 727–738.
[107] T.-C. Che, H.-F. Duan, P.J. Lee, Transient wave-based methods for anomaly detection in fluid pipes: A review, Mech. Syst. Signal Process. 160 (2021) 107874.
[108] M. Louati, M.S. Ghidaoui, High-frequency acoustic wave properties in a water-filled pipe. Part 1: Dispersion and multi-path behaviour, J. Hydraul. Res. 55 (5) (2017) 613–631.
[109] M. Louati, M.S. Ghidaoui, High-frequency acoustic wave properties in a water-filled pipe. Part 2: range of propagation, J. Hydraul. Res. 55 (5) (2017) 632–646.
[110] S. Nasraoui, M. Louati, M.S. Ghidaoui, Blockage detection in pressurized water-filled pipe using high frequency acoustic waves, Mech. Syst. Signal Process. 185 (2023) 109817.
[111] S.T. Peters, Composite Filament Winding, ASM International, 2011.
[112] C. Materials, Filament winding by CORE materials — Flicker images, 2011, [Online; accessed 17-September-2023].
[113] W. Commons, File:Oblique longitudinal-transverse winding.jpg — Wikimedia commons, the free media repository, 2020, [Online; accessed 17-September-2023].
[114] K. Paggioli, Centrifugally cast fiberglass-reinforced polymer mortar pipe for a large-diameter interceptor sewer, Mater. Perform. 45 (1) (2006) 58–61.
[115] C. Materials, Pultrusion by CORE materials — Flicker images, 2011, [Online; accessed 17-September-2023].